

Applied Mathematics & Information Sciences An International Journal

http://dx.doi.org/10.18576/amis/200105

Burr III Scaled Inverse Odds Ratio-Rayleigh Distribution for Modeling Asymmetric Engineering, Disease Surveillance and Epidemiological Data

Okechukwu J. Obulezi¹, Sadia Nadir², Gabriel O. Orji¹, Chinyere P. Igbokwe³, Gaber Sallam Salem Abdalla⁴, Abdoulie Faal^{5,*} and Mohammed Elgarhy⁶

Received: 7 Jul. 2025, Revised: 21 Sep. 2025, Accepted: 23 Oct. 2025

Published online: 1 Jan. 2026

Abstract: Reliability and epidemiology data in practice are of the type that require flexible distributions that fit heavy tails and varying hazard rates, which classical models like the Rayleigh distribution are not capable of. This work introduces the Burr III Scaled Inverse Odds Ratio-Rayleigh (B-SIOR-R) model, a novel model that overcomes such drawbacks. Our model, through the integration of Burr III scaling and inverse odds ratio transformation, provides more control over tail shapes, skewness, and hazards. We derive its statistical properties and estimate its parameters using the maximum likelihood method, which is affirmed by simulation studies. Our Monte Carlo simulations reveal the reduction and convergence towards zero of the bias and mean square error of the estimators with an increase in the sample size, where larger values show more stability and closer estimates to actual parameter values. We also derive a new group acceptance sampling plan (GASP) based on the B-SIOR-R model for quality control. The GASP results indicate that with an increasing true mean lifetime, the number of groups (g) and items in groups (m) to be sampled is reduced. For instance, using a consumer protection level 0.05 for β and a relative mean lifetime of 6 for r_2 , an optimal solution of $(g, m, P_{accept}) = (1, 1, 0.958898)$ is achieved, demonstrating an extremely satisfactory acceptance probability of around 95.89% by testing one group of one item. Within the practical applications, B-SIOR-R distribution generated evenly high p-values for all datasets—0.9900, 0.9543, 0.9965, 0.9966, and 0.3105—demonstrating its statistical sufficiency and robustness. Exactly, for the COVID-19 Mortality and HIV/AIDS Mortality datasets, B-SIOR-R model attained low AIC values (-240.94 and -27.45, respectively), outperforming most of the competitors in goodness-of-fit tests.

Keywords: Asymmetric data, Burr III distribution, Group Acceptance Sampling Plan (GASP), Inverse odds ratio, Rayleigh distribution, Hazard rate function.

1 Introduction

The Burr III scaled inverse odds ratio (B-SIOR-G) family has been recently introduced as a useful method of providing flexibility to baseline distributions. This is achieved by pairing the inverse odds ratio (IOR)

transformation with Burr III scaling. The IOR approach has attracted growing attention in the statistical literature due to its capability to generate distributions with improved skewness, kurtosis, and tail behavior. For instance, the inverse odds ratio-G (IOR-G) family [3] and

¹Department of Statistics, Faculty of Physical Sciences, Nnamdi Azikiwe University, P.O. Box 5025 Awka, Nigeria

²Department of Mathematics and Statistics, Faculty of Engineering and Applied Sciences, Riphah International University, Islamabad, Pakistan

³Department of Statistics, School of Computer Science and Engineering, Lovely Professional University, Phagwara, Punjab, 144411, India

⁴Department of Insurance and Risk Management, College of Business, Imam Mohammad Ibn Saud Islamic University (IMSIU), Riyadh, 11432, Saudi Arabia

⁵Mathematics Unit, Department Physical and Natural Sciences, School of Arts and Sciences, University of The Gambia, Faraba Campus, The Gambia

⁶Mathematics and Computer Science Department, Faculty of Science, Beni-Suef University, Egypt

^{*} Corresponding author e-mail: faala2520@gmail.com



its extensions have been demonstrated to provide a better fit than classical models for real data.

The B-SIOR-G family takes it a step further by introducing Burr III scaling into the IOR transformation. The introduction of Burr III scaling offers additional shape parameters that allow greater control over the tail thickness and the hazard rate function behavior. In this paper, we take a specific member of the B-SIOR-G family—the Burr III scaled inverse odds ratio-Rayleigh (B-SIOR-R) distribution. The new model is a generalization of the classical Rayleigh distribution, which has widespread use in engineering, survival analysis, and wireless communication due to its tractability and closed-form solutions. However, the default Rayleigh model assumes a monotonically increasing hazard rate, limiting its applicability in real-world applications requiring more flexibility in tail and hazard rate shape. The proposed B-SIOR-R model circumvents these limitations via the addition of three additional shape parameters. These allow the distribution to capture asymmetric shapes, heavier tails, and a wide range of hazard rate shapes including bathtub-shaped, unimodal, increasing, and quasi-normal forms. This makes the model extremely suitable for complex reliability, biomedical, and environmental data.

Flexible probability distributions are crucial to devise in engineering and reliability disciplines to represent lifetime and failure-time data in a precise manner. Classical models such as the exponential, Weibull, and Rayleigh distributions are commonly used because of their simplicity and interpretability. However, they are often not sufficient when the data exhibit heavy-tailed behavior, skewness, or non-monotonic hazard rates. To overcome such restrictions, several generalizations have been proposed, including the beta-G, Kumaraswamy-G, and transmuted-G families, which gain more flexibility by incorporating shape parameters [13], [14], [15]. Among them, the Burr family and most notably Burr Type III has gained popularity due to its capability to fit a myriad of hazard rate patterns and distributional shapes [16], [17]. The increasing complexity of real-life lifetime data has also provoked an increase in hybrid and compounded models, which often take advantage of transformation techniques like the odds ratio, inverse odds ratio, and T-X families for greater flexibility [18], [19]. Further references for readers are [29], [30], [31], [32], [33] and [34].

In epidemiology and disease surveillance, similar problems are faced in modeling mortality and survival rates. Classical models such as the log-normal, gamma, and Gompertz distributions cannot capture right-skewness, over-dispersion, and unusual hazard patterns in health data [20], [21]. Accordingly, recent studies have developed extended families with targeted application to public health. The IOR-G family, for example, has shown better fit to both HIV/AIDS mortality and COVID-19 survival data [1], [22].

Group acceptance sampling plans (GASP) are now essential tools in reliability testing and quality control when making decisions with small samples and under cost or time constraints. As opposed to single or double sampling plans, GASP takes groups of items together, making the decisions more effective and the inspection time less [23], [24]. Over the past decades, numerous researchers have developed GASP models under various lifetime distributions, including the Weibull, gamma, and exponential families [25], [24], [26]. More recently, GASP designs have been extended to generalized and flexible distributions for their wider applicability to real-life data with skewness, heavy tails, or complex hazard behavior [27], [28]. Motivated by all such developments, we develop a GASP under the proposed B-SIOR-R distribution. Since the model has the flexibility to accommodate various lifetime features, it provides a useful platform for developing effective sampling plans for use in industrial, biomedical, and reliability applications.

Data in fields like reliability and epidemiology often require flexible distributions that allow for heavy tails and various hazard rates, not provided by standard models like the Rayleigh distribution. In this article, a new distribution called the Burr III Scaled Inverse Odds Ratio-Rayleigh (B-SIOR-R) is introduced beyond these shortcomings. The main driving force is to address a deficit in statistical modeling through providing a more responsive instrument that more closely fits the full-fledged nature of data complexity. Through innovative integration of Burr III scaling and inverse odds ratio transformation, the model enjoys greater control over tail weight, skewness, and kurtosis, which is a valuable addition to the literature. In application, this research provides two main benefits: it enables improved fitting of complex asymmetric data, providing more trustworthy analysis, and it affords a tangible means of quality control through the creation of a new group acceptance sampling plan (GASP). The obvious benefits of improved data fitting and the development of a useful industrial instrument provide an effective case for its construction and illustrate its value.

The organization of the rest of this article is as follows; Section 2 specifies the Burr III Scaled Inverse Odd Ratio-Rayleigh (B-SIOR-R) distribution. In Section 3, the statistical properties of the B-SIOR-R distribution are studied. Section 4 dwells on parameter estimation using maximum likelihood approach. We designed a group acceptance sampling plan for truncated life tests based on the B-SIOR-R distribution for quality control in Section 5. A comprehensive Monte Calo simulation is carried out in Section 6. We deployed the proposed B-SIOR-R distribution to lifetime events in Section 7. Three datasets including groundwater measurement, Guage measurement, HIV/AIDs mortality, COVID-19 mortality, and COVID-19 survival rates were used to show that the new model is competitively better than some standard models in the literature. The article



was concluded with final remarks and future work in Section 8.

2 Specification of the new distribution

[1] created the Burr III scaled inverse odds ratio-G (B-SIOR-G) family of distributions with cumulative distribution function (CDF) given as

$$F_{\text{B-SIOR-R}}(x) = \left(1 + a \left[\frac{G(x; \boldsymbol{\omega})}{\bar{G}(x; \boldsymbol{\omega})}\right]^{-b}\right)^{-k}$$

$$= \left(1 + a \left[\frac{\bar{G}(x; \boldsymbol{\omega})}{G(x; \boldsymbol{\omega})}\right]^{b}\right)^{-k}; \quad x \in \mathbb{R},$$
(1)

where a,b,k>0 and ω is the parameter vector of any baseline distribution with CDF and survival function (SF) given as $G(x; \omega)$ and $\bar{G}(x; \omega)$ respectively. corresponding probability density function (PDF) is

$$f_{\text{B-SIOR-R}}(x) = abk \cdot g(x; \omega) \frac{\bar{G}(x; \omega)^{b-1}}{G(x; \omega)^{b+1}} \times \left(1 + a \left[\frac{\bar{G}(x; \omega)}{G(x; \omega)}\right]^{b}\right)^{-k-1}.$$
(2)

For any given parent distribution $G(x; \omega)$, the B-SIOR-G adds three additional parameters to its inverse odds ratio function and potentially provides a more robust and flexible model with a better goodness of fit. The B-SIOR-G family transforms the parent distributions' tails and increases the form of the hazard function (HF) associated with these baseline distributions. In the following part, we will examine a unique example within the B-SIOR-G family of distributions called the Burr III scaled odds ratio-Weibull (B-SIOR-W) inverse distribution.

of improving any baseline distribution, we introduce the Rayleigh distribution due to [2] into equations (1) and (2). The CDF, SF, and PDF of the Rayleigh distribution are defined respectively as $G(x;\omega)=1-e^{-\frac{x^2}{2\sigma^2}},$ $\bar{G}(x;\omega)=e^{-\frac{x^2}{2\sigma^2}},$ and $g(x;\omega)=\frac{x}{\sigma^2}e^{-\frac{x^2}{2\sigma^2}},$ where $\sigma>0.$ Plugging these into the CDF and PDF of the B-SIOR-G

To demonstrate that the B-SIOR-G family is capable

family, we obtain the CDF and PDF of the B-SIOR-R distribution given as

$$F_{\text{B-SIOR-R}}(x) = \left(1 + a \left[e^{\frac{x^2}{2\sigma^2}} - 1\right]^{-b}\right)^{-k}; \quad x \ge 0,$$

$$a, b, k, \sigma > 0.$$
 (3)

and

$$f_{\text{B-SIOR-R}}(x) = \frac{abk \, x}{\sigma^2} e^{-\frac{bx^2}{2\sigma^2}} \left(1 - e^{-\frac{x^2}{2\sigma^2}} \right)^{-b-1} \times \left(1 + a \left[e^{\frac{x^2}{2\sigma^2}} - 1 \right]^{-b} \right)^{-k-1}; \quad x \ge 0,$$
(4)

where k controls the steepness or decay. a, b and k are the shape parameters while σ is the scale parameter. For the B-SIOR-R distribution with PDF given in equation (4) and CDF in equation (3), the hazard function is given by

$$\begin{split} h_{\text{B-SIOR-R}}(x) &= \frac{abkx}{\sigma^2} e^{-\frac{bx^2}{2\sigma^2}} \left(1 - e^{-\frac{x^2}{2\sigma^2}} \right)^{-b-1} \\ &1 - \left(1 + a \left[e^{\frac{x^2}{2\sigma^2}} - 1 \right]^{-b} \right)^{-k} \\ &\times \left(1 + a \left[e^{\frac{x^2}{2\sigma^2}} - 1 \right]^{-b} \right)^{-k-1}; \quad x \geq 0. \end{split}$$

The B-SIOR-R distribution introduces additional flexibility to the classical Rayleigh distribution by modifying its tail behavior and hazard rate function, thereby allowing for better modeling of real-world phenomena characterized by skewness, heavy tails, and various hazard rate shapes.

2.1 Linear form of the density function

Consider using the following series identities $e^{-x} = \sum_{i=0}^{\infty} (-1)^i \frac{x^i}{i!}, \quad (1 - x)^{-n} = \sum_{j=0}^{\infty} {n+j-1 \choose j} x^j,$ $(1 + x)^{-n} = \sum_{h=0}^{\infty} (-1)^h {n+h-1 \choose h} x^h$ $(x-1)^{-n} = \sum_{r=0}^{\infty} {n+r-1 \choose r} x^r$, for |x| < 1 and n > 0, then the PDF in equation (4) can be decomposed in a more compact and tractable form as

$$f_{\text{B-SIOR-R}}(x) = k \sum_{i=0}^{\infty} \sum_{j=0}^{\infty} \sum_{h=0}^{\infty} \sum_{r=0}^{\infty} \frac{(-1)^{i+h}}{i!} \binom{b+j}{j}$$

$$\times \binom{k+h}{h} \binom{hb+r-1}{r} \frac{a^{h+1}b^{i+1}}{2^{i}\sigma^{2(i+1)}}$$

$$\times x^{2(i+1)} e^{-\frac{1}{2\sigma^{2}}(j-1)x^{2}}.$$
(5)

Figure (1) represents the graph of the PDF at various combination of the parameter values. The plots reflect leftskewed behaviour, both low and high peaks, and bumpedshape. This demonstrate that the B-SIOR-R can be utilized in modeling different lifetime events.

The hazard rate plots in Figure (2) depict bump-shape, bathtub, L-shape, J-shape and strictly non-decreasing shape. This again implies that B-SIOR-R model can benefit from modeling different lifetime events.



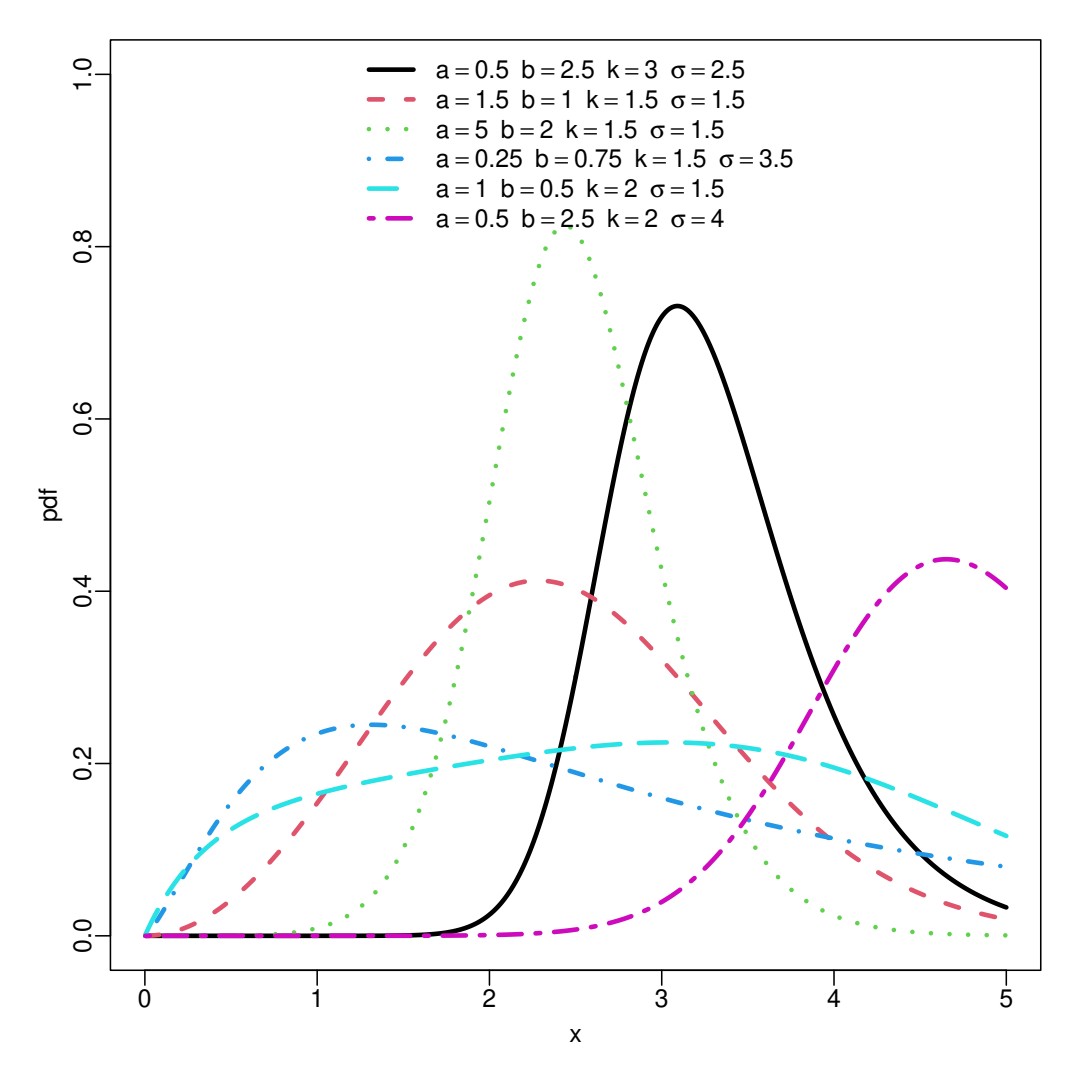


Fig. 1: PDF plots

3 Statistical Properties

A number of the essential properties of the proposed distribution are discussed in this section. Among them are the quantile function, the moment, moment generating function, mean residual life function, order statistic, and entropy.

3.1 Quantile Function

The quantile function plays a fundamental role in random variate generation, statistical inference, and reliability analysis. It provides an explicit expression for data values at specified cumulative probabilities. One of the most common techniques for deriving the quantile function is the probability integral transform, which converts a uniform random variable $U \sim \mathcal{U}(0,1)$ to the target distribution via the inverse of its CDF.

Let $x_u = F^{-1}(u)$ denote the quantile function of the B-SIOR-R distribution, where 0 < u < 1. Inverting the above cumulative distribution function, we get the following closed-form expression:

$$x_{u} = F^{-1}(u) = \sigma \sqrt{2 \ln \left\{ 1 + \left(\frac{a}{1 - \left(\frac{1}{u} \right)^{\frac{1}{k}}} \right)^{\frac{1}{b}} \right\}}; \quad 0 < u < 1.$$
(6)

This expression enables straightforward generation of B-SIOR-R random variables from uniform inputs and analytical computation of percentiles, medians, and thresholds required in practical applications such as acceptance sampling and risk analysis.



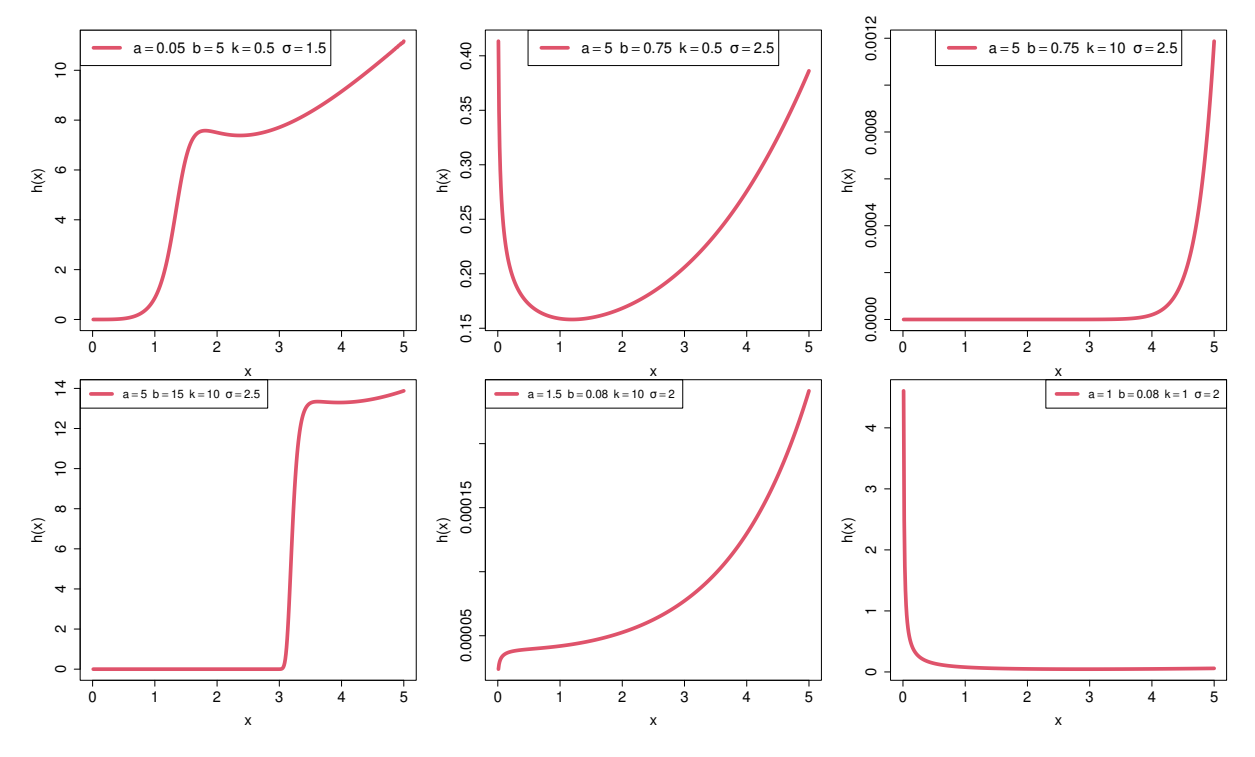


Fig. 2: Hazard Function Plots

3.2 Crude Moment

The $\omega - th$ crude moment for a continuous random variable with assumes the proposed B-SIOR-R distribution is defined as;

$$\begin{split} \mu_{\omega}' &= \int_{0}^{\infty} x^{\omega} f(x) \, dx \\ &= k \sum_{i=0}^{\infty} \sum_{j=0}^{\infty} \sum_{h=0}^{\infty} \sum_{r=0}^{\infty} \frac{(-1)^{i+h}}{i!} \binom{b+j}{j} \binom{k+h}{h} \\ &\times \binom{hb+r-1}{r} \frac{a^{h+1}b^{i+1}}{2^{i}\sigma^{2(i+1)}} \int_{0}^{\infty} x^{\omega+2(i+1)} \\ &\times e^{-\frac{1}{2}\sigma^{2}(j-1)x^{2}} dx. \end{split}$$

When a change of variable is made say $v = \omega + 2(i+1)$ and $\lambda = \frac{1}{2\sigma^2}(j-1)$, the integral becomes,

$$\int_0^\infty x^{\nu} e^{-\lambda x^2} dx = \frac{1}{2} \lambda^{-\frac{\nu+1}{2}} \Gamma\left(\frac{\nu+1}{2}\right), \quad \text{for } \lambda > 0.$$

This requires j > 1 so that $\lambda > 0$. If j = 0 or j = 1, the integral diverges — so the domain of summation should be from j = 2 to ∞ .

$$\mu_{\omega}' = k \sum_{i=0}^{\infty} \sum_{j=2}^{\infty} \sum_{h=0}^{\infty} \sum_{r=0}^{\infty} \frac{(-1)^{i+h}}{i!} \binom{b+j}{j} \binom{k+h}{h}$$

$$\times \binom{hb+r-1}{r} \frac{a^{h+1}b^{i+1}}{2^{i+1}\sigma^{2(i+1)}}$$

$$\times \left(\frac{1}{2\sigma^{2}}(j-1)\right)^{-\frac{\omega+2(i+1)+1}{2}}$$

$$\times \Gamma\left(\frac{\omega+2(i+1)+1}{2}\right). \tag{7}$$

Equation (7) is the ω th crude moment of the B-SIOR-R distribution in closed form. The convergence depends on the parameters a, b, k, σ and values of $j \ge 2$.

3.3 Incomplete Moment

Let $X \sim \text{B-SIOR-R}(a, b, k, \sigma)$. The ω -th incomplete moment evaluated at t > 0 is defined as

$$\mu_{\omega}'(t) = \int_0^t x^{\omega} f(x) \, dx.$$

Using the series expansion of the PDF, this becomes,



$$\begin{split} \mu_{\omega}'(t) &= k \sum_{i=0}^{\infty} \sum_{j=0}^{\infty} \sum_{h=0}^{\infty} \sum_{r=0}^{\infty} \frac{(-1)^{i+h}}{i!} \binom{b+j}{j} \binom{k+h}{h} \\ &\times \binom{hb+r-1}{r} \frac{a^{h+1}b^{i+1}}{2^{i}\sigma^{2(i+1)}} \\ &\times \int_{0}^{t} x^{\omega+2(i+1)} e^{-\frac{1}{2\sigma^{2}}(j-1)x^{2}} dx. \end{split}$$

Define

$$v = \omega + 2(i+1), \quad \lambda = \frac{1}{2\sigma^2}(j-1).$$

Then the integral can be expressed using the lower incomplete gamma function $\gamma(s,x)$ as

$$\int_0^t x^{\nu} e^{-\lambda x^2} dx = \begin{cases} \frac{1}{2} \lambda^{-\frac{\nu+1}{2}} \gamma\left(\frac{\nu+1}{2}, \lambda t^2\right), & \lambda > 0, \\ \frac{t^{\nu+1}}{\nu+1}, & \lambda = 0. \end{cases}$$

Since $\lambda > 0$ requires $j \ge 2$, the summation over j starts from 2 to ensure convergence. Hence, the incomplete moment is

$$\mu_{\omega}'(t) = k \sum_{i=0}^{\infty} \sum_{j=2}^{\infty} \sum_{h=0}^{\infty} \sum_{r=0}^{\infty} \frac{(-1)^{i+h}}{i!} \binom{b+j}{j} \binom{k+h}{h}$$

$$\times \binom{hb+r-1}{r} \frac{a^{h+1}b^{i+1}}{2^{i+1}\sigma^{2(i+1)}} \left(\frac{1}{2\sigma^{2}}(j-1)\right)^{-\frac{\nu+1}{2}}$$

$$\times \gamma \left(\frac{\nu+1}{2}, \frac{1}{2\sigma^{2}}(j-1)t^{2}\right). \tag{8}$$

When $t \to \infty$, $\gamma(s,x) \to \Gamma(s)$ and (8) reduces to the crude moment formula.

Figure (3) contain the plots of the Mean, Variance, Skewness and Kurtosis, illustrating the robustness of the B-SIOR-R distribution. The figures illustrate the behavior of the B-SIOR-R distribution's first four moments as parameters α and θ vary. Figure (a) displays the mean, showing a generally increasing trend with α and θ , indicating that larger values of these parameters lead to higher average values of the distribution. Figure (b) depicts the variance, which appears to decrease as both α and θ increase, suggesting reduced variability in the distribution for higher parameter values. Figure (c) presents the skewness, revealing a predominantly positive skewness across the parameter space, implying that the distribution is right-tailed. Notably, the skewness appears to decrease as α increases, particularly for larger values of θ . Lastly, Figure (d) illustrates the kurtosis, which consistently exhibits values greater than 3 (the kurtosis of a normal distribution), indicating that the B-SIOR-R distribution has heavier tails and a sharper peak than a normal distribution, suggesting a higher propensity for extreme values.

3.4 Moment Generating Function

Let X be a real-valued random variable. For any $t \in \mathbb{R}$, the moment generating function (MGF), written as $M_X(t)$ is defined as $M_X(t) = \mathbb{E}\left[e^{Xt}\right] = \int\limits_{-\infty}^{\infty} e^{tx} f_X(x) dx$. Given the PDF in equation (5), the MGF is

$$\begin{split} M_X(t) &= k \sum_{i=0}^{\infty} \sum_{j=0}^{\infty} \sum_{h=0}^{\infty} \sum_{r=0}^{\infty} \frac{(-1)^{i+h}}{i!} \binom{b+j}{j} \binom{k+h}{h} \\ &\times \binom{hb+r-1}{r} \frac{a^{h+1}b^{i+1}}{2^i \sigma^{2(i+1)}} \\ &\times \int_0^{\infty} x^{2(i+1)} e^{xt} e^{-\frac{1}{2\sigma^2}(j-1)x^2} \, dx. \end{split}$$

We can further reduce the form since $e^{xt} = \sum_{q=0}^{\infty} \frac{x^q}{q!}$, so that

$$\begin{split} M_X(t) &= k \sum_{i=0}^{\infty} \sum_{j=0}^{\infty} \sum_{h=0}^{\infty} \sum_{r=0}^{\infty} \sum_{q=0}^{\infty} \frac{(-1)^{i+h}}{i!q!} \binom{b+j}{j} \binom{k+h}{h} \\ &\times \binom{hb+r-1}{r} \frac{a^{h+1}b^{i+1}}{2^i \sigma^{2(i+1)}} \\ &\times \int_{0}^{\infty} x^{2(i+1)+q} e^{-\frac{1}{2\sigma^2}(j-1)x^2} \, dx. \end{split}$$

Let, v = 2(i+1) + q; $\lambda = \frac{1}{2\sigma^2}(j-1)$. Then the integral becomes,

$$\int_0^\infty x^{\nu} e^{-\lambda x^2} dx = \begin{cases} \frac{1}{2} \lambda^{-\frac{\nu+1}{2}} \Gamma\left(\frac{\nu+1}{2}\right), & \text{if } \lambda > 0\\ \infty, & \text{if } \lambda \le 0. \end{cases}$$

So we must restrict the index $j \ge 2$ to ensure $\lambda > 0$.

$$\begin{split} M_{X}(t) &= k \sum_{i=0}^{\infty} \sum_{j=2}^{\infty} \sum_{h=0}^{\infty} \sum_{r=0}^{\infty} \sum_{q=0}^{\infty} \frac{(-1)^{i+h}}{i!q!} \binom{b+j}{j} \binom{k+h}{h} \\ &\times \binom{hb+r-1}{r} \frac{a^{h+1}b^{i+1}}{2^{i+1}\sigma^{2(i+1)}} t^{q} \left(\frac{1}{2\sigma^{2}}(j-1)\right)^{-\frac{2(i+1)+q+1}{2}} \\ &\times \Gamma\left(\frac{2(i+1)+q+1}{2}\right). \end{split} \tag{9}$$

3.5 Mean Residual Life Function

The mean residual life (MRL) function at time *t* is defined as:



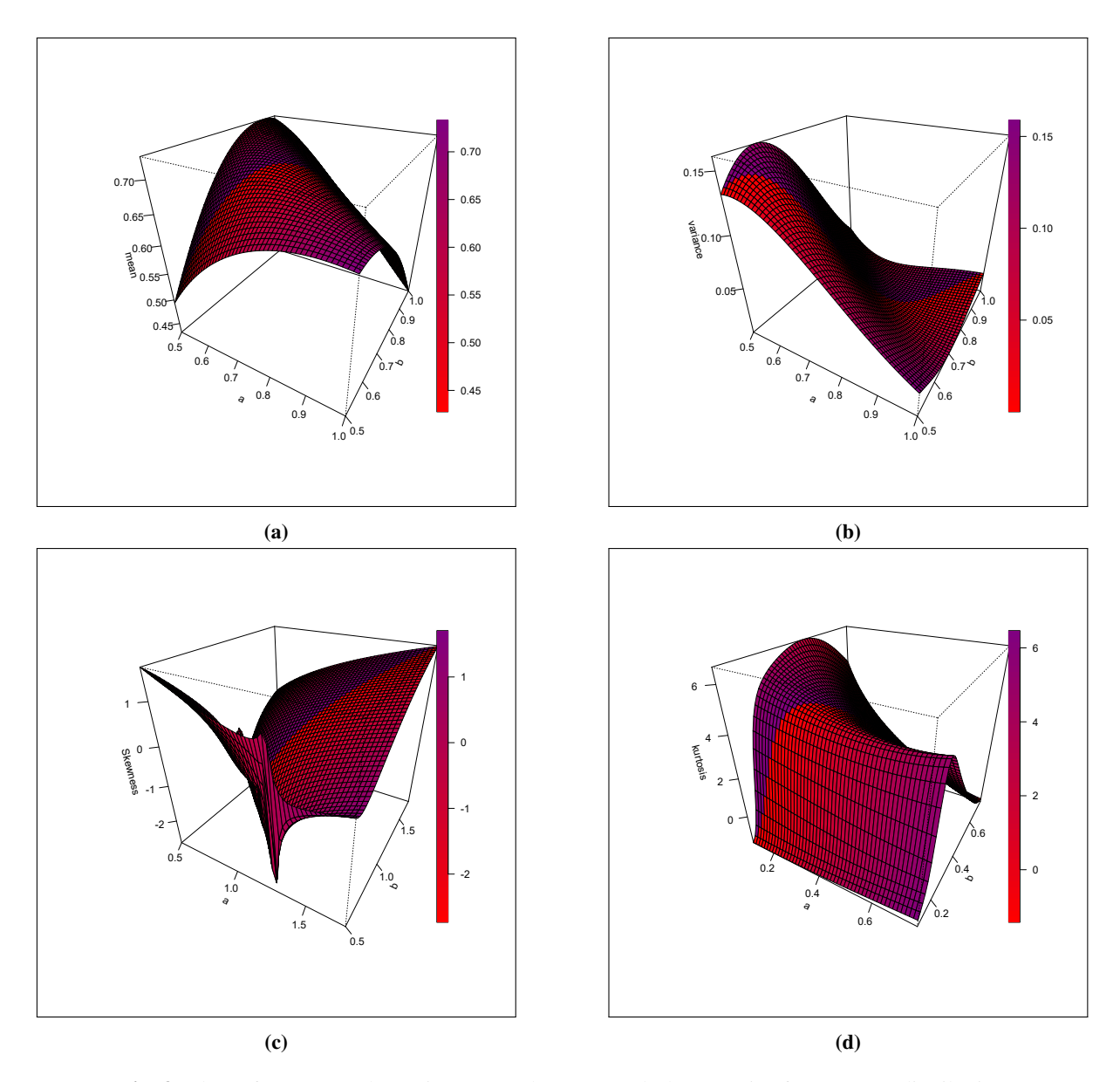


Fig. 3: Plots of (a) Mean, (b) Variance, (c) Skewness and (d) Kurtosis of B-SIOR-R distribution

$$m(t) = \mathbb{E}[X - t \mid X > t] \qquad (x - 1)^{-n} = \sum_{i=0}^{\infty} (-1)^{i} {n+i-1 \choose i} x^{i} \qquad \text{and}$$

$$m(t) = \mathbb{E}[X - t \mid X > t] \qquad (x - 1)^{-n} = \sum_{j=0}^{\infty} {n+j-1 \choose j} x^{j}, \text{ then}$$

$$= \frac{1}{1 - F(t)} \int_{t}^{\infty} (1 - F(x)) dx = \frac{1}{1 - \left(1 + a \left[e^{\frac{t^{2}}{2\sigma^{2}}} - 1\right]^{-b}\right)^{-k}} \qquad m(t) = \frac{1}{1 - \left(1 + a \left[e^{\frac{t^{2}}{2\sigma^{2}}} - 1\right]^{-b}\right)^{-k}}$$

$$\times \int_{t}^{\infty} \left[1 - \left(1 + a \left[e^{\frac{x^{2}}{2\sigma^{2}}} - 1\right]^{-b}\right)^{-k}\right] dx. \qquad \times \int_{t}^{\infty} \left[1 - \sum_{i=0}^{\infty} \sum_{j=0}^{\infty} (-1)^{i} {k+i-1 \choose i} \right] dx. \qquad (10)$$
Using binomial expansion identities namely;



Equation (10) is completely resolved by numerically computation.

3.6 Order Statistic

Let $X_{r:n}$ denote the rth order statistic in a random sample of size n from a continuous distribution, then the PDF of $X_{r:n}$ is:

$$f_{X_{r:n}}(x) = \frac{n!}{(r-1)!(n-r)!} [F(x)]^{r-1} [1 - F(x)]^{n-r} f(x).$$

Using equations (3) and (4)

$$f_{X_{r,n}}(x) = \frac{n!}{(r-1)!(n-r)!} \left[\left(1 + a \left(e^{\frac{x^2}{2\sigma^2}} - 1 \right)^{-b} \right)^{-k} \right]^{r-1} \\ \times \left[1 - \left(1 + a \left(e^{\frac{x^2}{2\sigma^2}} - 1 \right)^{-b} \right)^{-k} \right]^{n-r} \frac{abkx}{\sigma^2} e^{-\frac{bx^2}{2\sigma^2}} \\ \times \left(1 - e^{-\frac{x^2}{2\sigma^2}} \right)^{-b-1} \left(1 + a \left(e^{\frac{x^2}{2\sigma^2}} - 1 \right)^{-b} \right)^{-k-1} .$$

Using the same set of binomial identities already stated in subsection 2.1,

$$f_{X_{r:n}}(x) = \frac{n!}{(r-1)!(n-r)!} \frac{abkx}{\sigma^2} \sum_{i=0}^{\infty} \sum_{j=0}^{\infty} (-1)^i \times \binom{k(r-1)+i-1}{i} \binom{ib+j-1}{j} \sum_{l=0}^{n-r} \times \sum_{m=0}^{\infty} \sum_{p=0}^{\infty} \sum_{q=0}^{\infty} (-1)^{l+m+q} \binom{n-r}{l} \binom{lk+m-1}{m}$$

$$\times \binom{mb+p-1}{p} \binom{b+q}{q} \sum_{s=0}^{\infty} \sum_{u=0}^{\infty} (-1)^s \binom{k+s}{s} \times \binom{sb+u-1}{u} a^{i+m+s} e^{-\frac{1}{2\sigma^2}(b+q-j-p-u)x^2}.$$
(11)

The smallest and largest PDF of the rth order statistic is obtained when r = 1 and r = n respectively.

3.7 Entropy

Entropy is the amount of information that is contained in an observation X. Higher entropy implies greater uncertainty or wider spread of the distribution while lower entropy implies less uncertainty or concentrated distribution. For a continuous random variable, the measure of Rény entropy is

$$H(X) = \frac{1}{1 - q} \log \left(\int_{-\infty}^{\infty} f^{q}(x) \, dx \right),$$

where $q \neq 1$ and q > 0. Therefore, using the PDF of the B-SIOR-R distribution,

$$\begin{split} H(X) &= \frac{1}{1-q} \log \left\{ \int_0^\infty \left(\frac{abk}{\sigma^2} \right)^q \left(1 - e^{-\frac{x^2}{2\sigma^2}} \right)^{-q(b+1)} \right. \\ & \left. x^q e^{-\frac{qbx^2}{2\sigma^2}} \left[1 + a \left(e^{\frac{x^2}{2\sigma^2}} - 1 \right)^{-b} \right]^{-q(k+1)} dx \right\} \\ &= \frac{1}{1-q} \log \left\{ \left(\frac{abk}{\sigma^2} \right)^q \sum_{i=0}^\infty \sum_{j=0}^\infty \sum_{w=0}^\infty (-1)^{i+j} \right. \\ & \times \left. \left(\frac{q(b+1) + i - 1}{i} \right) \left(\frac{q(k+1) + j - 1}{j} \right) \right. \\ & \times \left(\frac{jb + w - 1}{w} \right) a^j \int_0^\infty x^q e^{-\frac{1}{2\sigma^2} (qb + i - w)x^2} dx \right\}. \end{split}$$

Let,
$$m=q$$
 and $\lambda=\frac{1}{2\sigma^2}(qb+i-w)$, then;
$$\int_0^\infty x^q e^{-\frac{1}{2\sigma^2}(qb+i-w)x^2} \qquad dx = \frac{1}{2}\left(\frac{1}{2\sigma^2}(qb+i-w)\right)^{-\frac{q+1}{2}}\Gamma\left(\frac{q+1}{2}\right).$$
 Substituting this back gives

$$H(X) = \frac{1}{1-q} \log \left\{ \left(\frac{abk}{\sigma^2} \right)^q \frac{1}{2} \Gamma \left(\frac{q+1}{2} \right) \right.$$

$$\times \sum_{i=0}^{\infty} \sum_{j=0}^{\infty} \sum_{w=0}^{\infty} (-1)^{i+j} \binom{q(b+1)+i-1}{i}$$

$$\times \binom{q(k+1)+j-1}{j} \binom{jb+w-1}{w}$$

$$\times a^j \left(\frac{1}{2\sigma^2} (qb+i-w) \right)^{-\frac{q+1}{2}} \right\}.$$
(12)

3.8 Extropy

Extropy is a complementary measure to entropy, quantifying the uncertainty of a random variable from a different perspective. For a continuous random variable X with PDF f(x), the extropy is defined as

$$J(X) = -\frac{1}{2} \int_{-\infty}^{\infty} f^2(x) \, dx.$$

Using the PDF of the B-SIOR-R distribution, we have



$$\begin{split} J(X) &= -\frac{1}{2} \int_0^\infty \left[\frac{abk}{\sigma^2} x e^{-\frac{bx^2}{2\sigma^2}} \left(1 - e^{-\frac{x^2}{2\sigma^2}} \right)^{-b-1} \right. \\ &\times \left(1 + a \left(e^{\frac{x^2}{2\sigma^2}} - 1 \right)^{-b} \right)^{-k-1} \right]^2 dx \\ &= -\frac{1}{2} \left(\frac{abk}{\sigma^2} \right)^2 \int_0^\infty x^2 e^{-\frac{bx^2}{\sigma^2}} \left(1 - e^{-\frac{x^2}{2\sigma^2}} \right)^{-2(b+1)} \\ &\times \left(1 + a \left(e^{\frac{x^2}{2\sigma^2}} - 1 \right)^{-b} \right)^{-2(k+1)} dx. \end{split}$$

Expanding the negative powers using binomial and multinomial series expansions yields

$$\begin{split} J(X) &= -\frac{1}{2} \left(\frac{abk}{\sigma^2}\right)^2 \sum_{i=0}^{\infty} \sum_{j=0}^{\infty} \sum_{w=0}^{\infty} (-1)^{i+j} \binom{2(b+1)+i-1}{i} \\ &\times \binom{2(k+1)+j-1}{j} \binom{jb+w-1}{w} a^j \\ &\times \int_0^{\infty} x^2 e^{-\frac{1}{2\sigma^2}(2b+i-w)x^2} dx, \end{split}$$

where the integral can be evaluated as

$$\int_0^\infty x^2 e^{-\lambda x^2} dx = \frac{1}{2} \lambda^{-\frac{3}{2}} \Gamma\left(\frac{3}{2}\right), \quad \lambda > 0,$$

with $\lambda = \frac{1}{2\sigma^2}(2b+i-w)$. Substituting back, the extropy simplifies to

$$J(X) = -\frac{1}{4} \left(\frac{abk}{\sigma^2}\right)^2 \Gamma\left(\frac{3}{2}\right) \sum_{i=0}^{\infty} \sum_{j=0}^{\infty} \sum_{w=0}^{\infty} (-1)^{i+j} \times \binom{2(b+1)+i-1}{i} \binom{2(k+1)+j-1}{j} \times \binom{jb+w-1}{w} a^j \left(\frac{1}{2\sigma^2} (2b+i-w)\right)^{-\frac{3}{2}}.$$
 (13)

This provides a closed-form expression for the extropy of the B-SIOR-R distribution. The series converges under suitable parameter conditions.

4 Parameter Estimation

Let x_1, x_2, \dots, x_n be a random sample from the B-SIOR-R distribution with PDF defined in equation (4), then the likelihood function [35, 36, 37, 38, 39, 40] is given by

$$\begin{split} L(a,b,k,\sigma) &= \prod_{i=1}^n \frac{abkx}{\sigma^2} e^{-\frac{bx^2}{2\sigma^2}} \left(1 - e^{-\frac{x^2}{2\sigma^2}}\right)^{-b-1} \\ &\times \left(1 + a\left[e^{\frac{x^2}{2\sigma^2}} - 1\right]^{-b}\right)^{-k-1}. \end{split}$$

The log-likelihood is expressed as

$$\ell(a,b,k,\sigma) = n\log a + n\log b + n\log k - 2n\log \sigma + \sum_{i=1}^{n} \log x_{i} - \sum_{i=1}^{n} \frac{bx_{i}^{2}}{2\sigma^{2}} - (b+1) \sum_{i=1}^{n} \log \left(1 - e^{-\frac{x_{i}^{2}}{2\sigma^{2}}}\right) - (k+1) \sum_{i=1}^{n} \log \left(1 + a\left(e^{\frac{x_{i}^{2}}{2\sigma^{2}}} - 1\right)^{-b}\right).$$

The first partial derivative with respect to a is

$$\frac{\partial \ell}{\partial a} = \frac{n}{a} - (k+1) \sum_{i=1}^{n} \frac{\left(e^{\frac{x_i^2}{2\sigma^2}} - 1\right)^{-b}}{1 + a\left(e^{\frac{x_i^2}{2\sigma^2}} - 1\right)^{-b}}.$$

The first partial derivative with respect to b is

$$\frac{\partial \ell}{\partial b} = \frac{n}{b} - \sum_{i=1}^{n} \frac{x_i^2}{2\sigma^2} - \sum_{i=1}^{n} \log\left(1 - e^{-\frac{x_i^2}{2\sigma^2}}\right) + (k+1) \sum_{i=1}^{n} \frac{a\left(e^{\frac{x_i^2}{2\sigma^2}} - 1\right)^{-b} \log\left(e^{\frac{x_i^2}{2\sigma^2}} - 1\right)}{1 + a\left(e^{\frac{x_i^2}{2\sigma^2}} - 1\right)^{-b}}$$

The first partial derivative with respect to k is

$$\frac{\partial \ell}{\partial k} = \frac{n}{k} - \sum_{i=1}^{n} \log \left(1 + a \left(e^{\frac{x_i^2}{2\sigma^2}} - 1 \right)^{-b} \right)$$

Set
$$\frac{\partial \ell}{\partial \hat{k}} = 0$$
, then $\hat{k} = \frac{\sum\limits_{i=1}^{n} \log \left(1 + a \left(e^{\frac{x_i^2}{2\sigma^2} - 1}\right)^{-b}\right)}{n}$. The first partial derivative with respect to σ

$$\begin{split} &\frac{\partial \ell}{\partial \sigma} = (b+1) \sum_{i=1}^{n} \frac{\exp\left(-\frac{x_i^2}{2\sigma^2}\right) x_i^2}{\sigma^3 \left(1 - \exp\left(-\frac{x_i^2}{2\sigma^2}\right)\right)} \\ &+ (k+1) \sum_{i=1}^{n} \left[\frac{ab \left(\exp\left(\frac{x_i^2}{2\sigma^2}\right) - 1\right)^{-b-1} \exp\left(\frac{x_i^2}{2\sigma^2}\right)}{1 + a \left(\exp\left(\frac{x_i^2}{2\sigma^2}\right) - 1\right)^{-b}} \frac{x_i^2}{\sigma^3} \right] \\ &- \frac{2n}{\sigma} + b \sum_{i=1}^{n} \frac{x_i^2}{\sigma^3}. \end{split}$$

Setting $\frac{\partial \ell}{\partial a}=0$, $\frac{\partial \ell}{\partial b}=0$ and $\frac{\partial \ell}{\partial \sigma}=0$ lead to non-closed functional form requiring numerical computation technique to achieve convergence.



5 GASP design under the B-SIOR-R Model

The group acceptance sampling procedure (GASP) is designed to optimize the use of time and resources by reducing the number of required tests through an efficient sampling methodology. Prior to the acceptance or rejection of a lot, specific quality control tests are carried out under various sampling schemes.

This section presents an illustrative example of a GASP assuming that the lifetime of an item follows the distribution. The relevant distribution B-SIOR-R parameters include a, k, and b, with the CDF defined in equation (3). Randomized statistical methods are employed to evaluate the product's performance and reliability, offering valuable insights for assurance.

The GASP framework is structured to maximize the reliability assessment of the product, and involves the following key steps:

- (a) Select a total of *n* items at random and divide them into g groups of r items each. This implies $n = r \times g$, which is a fixed requirement.
- (b) Determine the test duration t_0 , and the acceptance number m, which serves as the threshold for allowable failures per group.
- (c) Conduct the experiment simultaneously across all g groups, and observe the number of failures in each
- (d) Accept the lot if each group records no more than mfailures.
- (e) Reject the lot immediately and entirely if any group exceeds m failures.

For a fixed group size r, the proposed GASP is fully specified by the design parameters g and m. The test termination time t_0 is determined as $t_0 = a_1 \mu_0$, where a_1 is a predetermined constant and μ_0 is the specified or expected median lifetime.

The probability of accepting the lot under this sampling plan is given by:

$$P_{accept}(p) = \left[\sum_{i=0}^{\mu} {r \choose i} p^{i} (1-p)^{r-i}\right]^{g},$$

where p denotes the probability that a single item fails before time t_0 .

The expression for the median lifetime of the B-SIOR-R distribution is provided in equation (14), while its CDF is given in equation (3). Let the median lifetime of an item which assumes the B-SIOR-R model be

$$\mu = \sigma \sqrt{2\ln\left\{1 + \left(\frac{a}{1 - \left(\frac{1}{u}\right)^{\frac{1}{k}}}\right)^{\frac{1}{b}}\right\}} \tag{14}$$

Then suppose we let

$$w = \sqrt{2\ln\left\{1 + \left(\frac{a}{1 - \left(\frac{1}{u}\right)^{\frac{1}{k}}}\right)^{\frac{1}{b}}\right\}}.$$

w is defined at u = 0.5, which represents the median lifetime. Hence

$$w = \sqrt{2\ln\left\{1 + \left(\frac{a}{1 - 2^{\frac{1}{k}}}\right)^{\frac{1}{b}}\right\}}.$$

This implies that $w = \frac{\mu}{\sigma}$ and $t_0 = a_1 \times \mu_0$. If these are replaced in the CDF in equation (3), then the probability of failure of an item is expressed as

$$p = \left[1 + a \left(e^{\frac{(a_1 \times w)^2}{2(r_2)^2}} - 1 \right)^{-b} \right]^{-k},$$

where $r_2 = \frac{\mu}{\mu_0}$. For given values of a, k, and b, the probability p can be computed when the parameters a_1 and r_2 are specified, where $r_2 = \frac{\mu}{\mu_0}$. The two failure probabilities considered are denoted by p_1 and p_2 , which correspond to the consumer and producer risks, respectively. To determine the design parameters g and mfor a given quality level and specified risks, the following optimization problem is formulated:

Minimize the Average Sample Number (ASN): $n = r \times$ g, subject to

$$P_{\text{accept}}(p_1 \mid \frac{\mu}{\mu_0} = r_1) = \left[\sum_{i=0}^{m} {r \choose i} p_1^i (1 - p_1)^{r-i} \right]^g \le \beta,$$
(15)

$$P_{\text{accept}}(p_2 \mid \frac{\mu}{\mu_0} = r_2) = \left[\sum_{i=0}^m \binom{r}{i} p_2^i (1 - p_2)^{r-i} \right]^g \ge 1 - \alpha.$$
(16)

Here, r_1 and r_2 denote the mean ratios associated with the consumer and producer risks, respectively. The failure probabilities p_1 and p_2 are evaluated within the acceptance probability functions P_{accept} in Equations (15) and (16).

Table (1) presents optimal parameter values for a Group Acceptance Sampling Plan (GASP) for the Burr-Scaled Inverse Odd Rayleigh Ratio (B-SIOR-R) distribution. The lifetime data are modelled using this distribution with constants: a = 0.25, b = 1.05, and k = 0.75. The sampling plan is designed for varying values of:

- (a) $\beta \in \{0.25, 0.10, 0.05, 0.01\}$: the consumer's risk,
- (b) $r_2 = \mu/\mu_0 \in \{2,4,6,8\}$: the true mean lifetime μ to the given mean μ_0 ,
- (c) $r \in \{5, 10\}$: number of inspection repetitions or rounds,



Table 1: GASP under B-SIOR-R at a = 0.25, b = 1.05, k = 0.75 and with minimum g and m

				r =	5						- 10		
β	$r_2 = \frac{\mu}{\mu_0}$		<i>a</i> ₁ =	= 0.5		а	$_{1} = 1$		a_1	= 0.5		a_1	= 1
	, ,	g	m	$P_{accept}(p)$	g	m	$P_{accept}(p)$	g	m	$P_{accept}(p)$	g	m	$P_{accept}(p)$
	2	24	3	0.96409	8	4	0.956429	5	4	0.968175	3	7	0.984427
0.25	4	2	1	0.959834	1	2	0.979715	2	2	0.980394	1	3	0.963695
0.23	6	2	1	0.988054	1	1	0.953286	1	1	0.975199	1	2	0.967607
	8	2	1	0.995054	1	1	0.979711	1	1	0.989435	1	2	0.990148
	2	414	4	0.980951	0	4	0	22	5	0.982335	5	7	0.974181
0.10	4	9	2	0.991201	2	2	0.959841	2	2	0.980394	1	3	0.963695
0.10	6	3	1	0.982134	1	1	0.953286	1	1	0.975199	1	2	0.967607
	8	3	1	0.99259	1	1	0.979711	1	1	0.989435	1	2	0.990148
	2	538	4	0.975316	0	4	0	29	5	0.97678	7	7	0.96404
0.05	4	11	2	0.989257	2	2	0.959841	3	2	0.970735	1	3	0.963695
0.03	6	4	1	0.97625	1	1	0.953286	2	1	0.951013	1	2	0.967607
	8	4	1	0.990133	1	1	0.979711	2	1	0.978982	1	2	0.990148
	2	827	4	0.962309	0	4	0	44	5	0.964982	28	8	0.983507
0.01	4	17	2	0.983445	7	3	0.98939	4	2	0.961172	2	4	0.987146
0.01	6	6	1	0.964587	3	2	0.989328	2	1	0.951013	1	2	0.967607
	8	6	1	0.985236	2	1	0.959834	2	1	0.978982	1	2	0.990148

(d) $a_1 \in \{0.5, 1\}$: shape parameter of the underlying prior distribution.

For every setting of the parameters, the GASP design is represented as a triplet $(g, m, P_{accept}(p))$, where:

g = number of groups to be inspected,

m = number of items in each group, $P_{\text{accept}}(p) =$ probability of accepting a lot when the true defect level is p.

The values of g and m are selected so that the acceptance probability satisfies the constraint:

$$P_{\text{accept}}(p) \ge 1 - \beta$$
,

where p is the ratio of nonconforming units in the lot. Following are the observation and trend;

- (i) For any β and a_1 , increasing the mean ratio r_2 (i.e., higher quality lots) will give smaller g and m, with lower sampling requirements more reliably.
- (ii) For smaller β (more risk-averse consumers), the values of g and/or m are higher, imposing stricter inspection in a way that maintains the acceptance probability at the preferred level.
- (iii) Higher values of the repetition factor r or the shape parameter a_1 may produce more frugal sampling plans (lower g or m), although this is not a purely monotonic pattern in all cases.
- (iv) g=0 values are invalid or nonpractical sampling plans, possibly implying automatic rejection or impossible settings given current conditions.

Figure 4 is the Operating Characteristic (OC) curve for a = 0.25, b = 1.05, k = 0.75. Panel 4a is when r = 5 and

 $a_1 = 0.5$, panel 4b is when r = 5 and $a_1 = 1$, panel 4c is when r = 10 and $a_1 = 0.5$, panel 4d is when r = 10 and $a_1 = 1$.

Table (2) displays the optimal designs for a GASP under B-SIOR-R distribution when the distributional parameters are fixed at $a=1.75,\,b=0.25,$ and k=2.75. Each row of the table corresponds to a specific set of:

- (a) $\beta \in \{0.25, 0.10, 0.05, 0.01\}$: the consumer's risk (Type II error),
- (b) $r_2 = \mu/\mu_0 \in \{2,4,6,8\}$: the ratio of the true mean lifetime μ to the nominal mean μ_0 ,
- (c) $r \in \{5, 10\}$: number of inspection repetitions (e.g., time units or stages),
- (d) $a_1 \in \{0.5, 1\}$: shape parameter for the sampling model.

For each configuration, the optimal GASP is designated by the triplet $(g, m, P_{accept}(p))$, where:

g= number of groups selected for inspection, m= number of items inspected in each group, $P_{\text{accept}}(p)=$

probability of accepting the lot at true defect proportion *p*. Design parameters *g* and *m* are chosen to minimize the cost of sampling (i.e., make *g* and *m* as small as possible) subject to the constraint that

$$P_{\text{accept}}(p) \ge 1 - \beta$$
.

The following are the key results from the outcome;

(i) As r_2 increases (i.e., the actual mean lifetime improves), both g and m go down, showing the effectiveness of GASP for good environments.



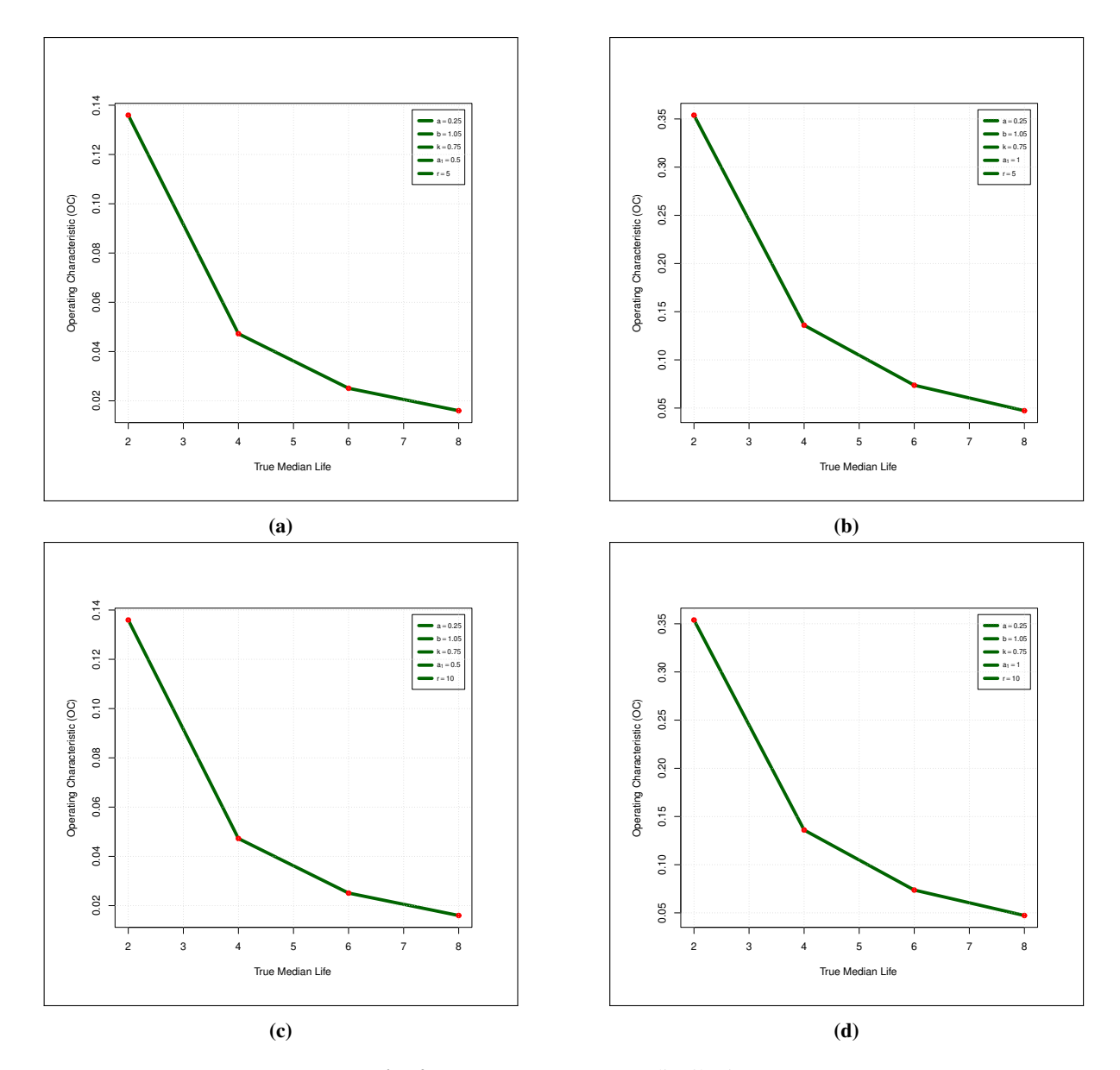


Fig. 4: OC Curves B-SIOR-R distribution

- (ii) Small β (e.g., 0.01) means stricter consumer protection, which usually requires a larger sample size g or m in order to obtain acceptable $P_{\rm accept}$.
- (iii) A degenerate case of g = 0 and $P_{\text{accept}} = 0$ indicates infeasibility i.e., such plans are non-operational or lead to automatic rejection due to excessive stringency under a given β .
- (iv) As r increases from 5 to 10, fewer groups are sometimes needed for the same or better acceptance probability especially when $a_1 = 1$. This means that more inspection repetition improves lot discriminability.
- (v) Shape parameter a_1 influences plan optimality: for instance, with $a_1 = 1$, g is minimized more than with

 $a_1 = 0.5$, which means that this shape parameter enhances sampling efficiency under the B-SIOR-R model.

For instance, for $\beta = 0.05$, $r_2 = 6$, r = 10, and $a_1 = 1$, the optimal plan is $(g, m, P_{\text{accept}}) = (1, 1, 0.958898)$, i.e., inspecting 1 group of 1 item, with a high acceptance probability of about 95.89

Figure 5 is the Operating Characteristic (OC) curve for a=1.75, b=0.25, k=2.75. Panel 5a is when r=5 and $a_1=0.5$, panel 5b is when r=5 and $a_1=1$, panel 5c is when r=10 and $a_1=0.5$, panel 5d is when r=10 and $a_1=1$.



Table 2: GASP under B-SIOI	R-R at $a = 1.7$:	5.b = 0.25.k =	= 2.75 and with	minimum ϱ and m

				r =	= 5					r =	10		
β	$r_2 = \frac{\mu}{\mu_0}$		<i>a</i> ₁ =	= 0.5		a_1	= 1		<i>a</i> ₁ =	= 0.5		а	$\frac{1}{1} = 1$
	. •	g	m	$P_{accept}(p)$	g	m	$P_{accept}(p)$	g	m	$P_{accept}(p)$	g	m	$P_{accept}(p)$
	2	986	3	0.966171	2	2	0.962054	41	3	0.952471	1	3	0.96608
0.25	4	72	2	0.990291	1	1	0.975709	10	2	0.985252	1	2	0.987232
0.23	6	10	1	0.976991	1	1	0.989808	3	1	0.970484	1	1	0.958898
	8	10	1	0.987713	1	1	0.994452	3	1	0.984019	1	1	0.976961
	2	0	4	0	7	3	0.990202	390	4	0.970618	1	3	0.96608
0.10	4	120	2	0.983871	2	1	0.952008	16	2	0.976507	1	2	0.987232
0.10	6	16	1	0.963441	2	1	0.979719	5	1	0.951293	1	1	0.958898
	8	16	1	0.980413	2	1	0.988936	5	1	0.973507	1	1	0.976961
	2	0	4	0	9	3	0.98742	508	4	0.9619	2	4	0.988252
0.05	4	155	2	0.979216	2	1	0.952008	21	2	0.96928	1	2	0.987232
0.05	6	21	1	0.952293	2	1	0.979719	21	2	0.991408	1	1	0.958898
	8	21	1	0.974372	2	1	0.988936	7	1	0.963107	1	1	0.976961
	2	0	4	0	14	3	0.9805	0	4	0	3	4	0.982431
0.01	4	239	2	0.968133	5	2	0.993542	31	2	0.954984	2	2	0.974627
0.01	6	239	2	0.991365	3	1	0.969734	31	2	0.987343	1	1	0.958898
	8	32	1	0.96121	3	1	0.98345	31	2	0.995031	1	1	0.976961

6 Simulations

In this subsection, we access the performance of the estimated parameters $\hat{a}, \hat{b}, \hat{k}, \hat{\sigma}$ with the aid of a simulation study (SimS). Using the inverse CDF approach to generate random numbers from the BSIORR distribution, the SimS procedure was carried out. We choose an adequate random sample from the B-SIOR-R distribution for the SimS. The following are two sets of parameters for running the SimS.

Set 1:
$$a = 0.5, b = 3.2, k = 1.5, \sigma = 1$$

Set 2: $a = 0.1, b = 2.5, k = 1, \sigma = 1$

The chosen parameters in the simulation section need to be assessed so that they can determine how those specific values will evaluate the expected performance of the B-SIOR-R distribution. The choice of the parameter values are based on the following reasons;

- To ensure a variety of hazard function Shapes, such as increasing, decreasing, and bathtub-shaped hazard functions.
- ii. The parameter values closely approach real-world distributions seen in reliability engineering, survival analysis, and failure time modeling.
- iii. Choosing intermediate values guarantees that the distribution has a realistic tail behavior while avoiding severe skewness or computational instability.
- iv. To further validate these decisions, a sensitivity analysis was conducted by adjusting one parameter at a time to see how MLE performs under different scenarios. This proved the estimating method's robustness over a wide range of parameter values.

Furthermore, the evaluation criteria namely Bias, Absolute Bias and Mean Square Error (MSE) were considered for assessing the performance of the model. These criteria are respectively computed with the help of the following expressions:

the following expressions:

Bias =
$$\frac{1}{1000} \sum_{i=1}^{1000} (\hat{w} - w);$$

Absolute Bias = $\frac{1}{1000} \sum_{i=1}^{1000} |(\hat{w} - w)|;$ and

 $MSE = \frac{1}{1000} \sum_{i=1}^{1000} (\hat{w} - w)^2.$

The simulation results for the B-SIOR-R model across varying sample sizes n provide insights into the behavior of the MLEs, biases, and Mean Squared Errors (MSEs) of the parameters a, b, k, and σ . The simulation study yielded the following important findings:

- 1.As the sample size increases, the estimators exhibit greater stability and converge more closely to the true parameter values.
- 2. The bias and mean square error of the estimators decrease with larger sample sizes, approaching zero.
- 1.For both parameter sets, the bias and MSE of all parameter estimates decrease as the sample size *n* increases, illustrating the consistency property of the MLE. That is,

$$\lim_{n\to\infty}\widehat{\theta}_n=\theta\quad\text{in probability,}$$

where $\widehat{\theta}_n$ denotes the MLE based on sample size n and θ is the true parameter value.



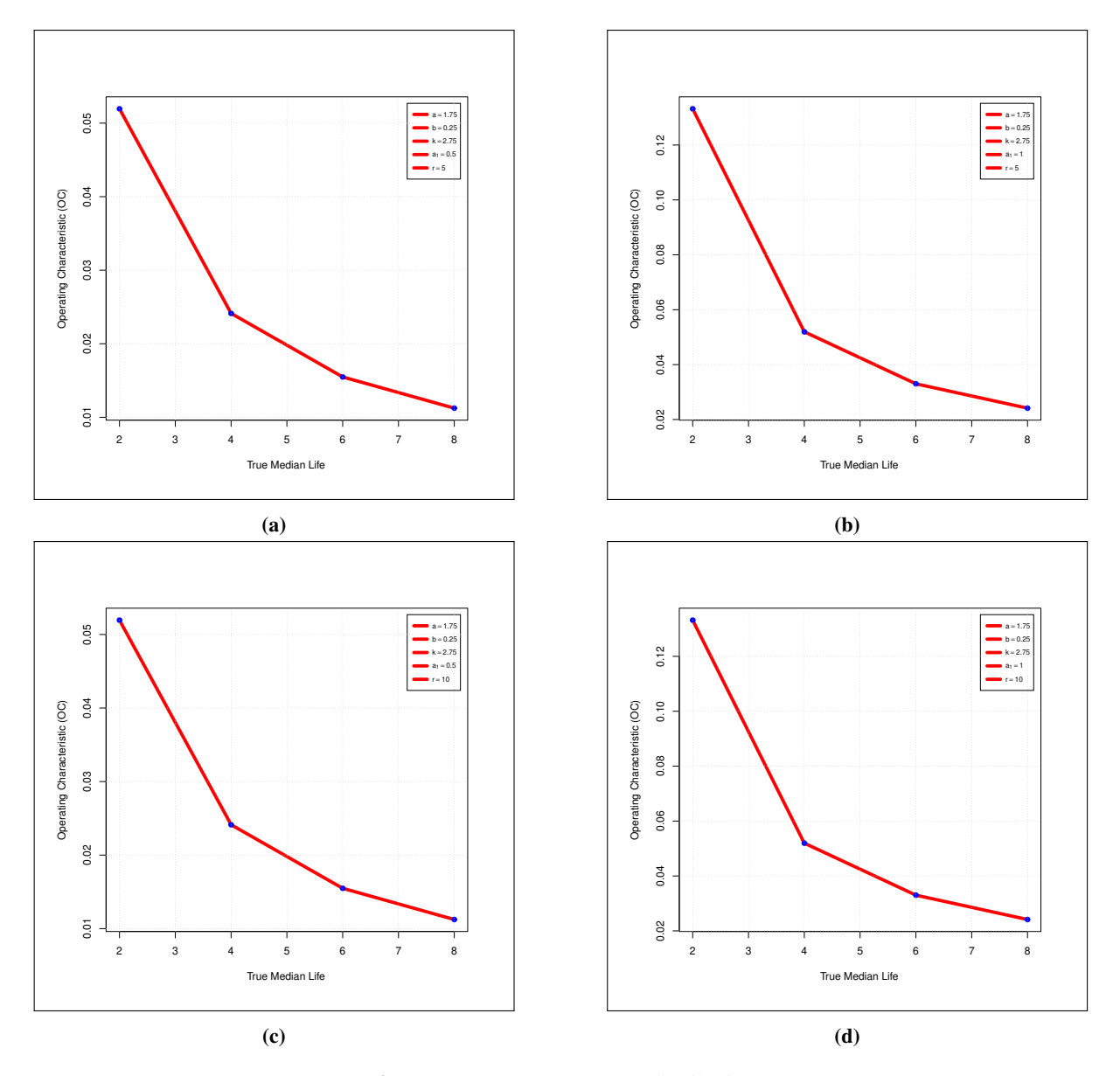


Fig. 5: OC Curves B-SIOR-R distribution

- 2. The parameter σ is estimated with relatively low bias and MSE even for small sample sizes, indicating its identifiability and stability under the model.
- 3.For Set 1 (with higher values of a, b, and k), the bias and MSE are generally larger at small n but reduce significantly as n increases. For instance, the MSE of \hat{k} decreases from 3.84 at n = 25 to about 0.056 at n = 900.
- 4.In contrast, Set 2, which has lower parameter values, exhibits better performance in terms of bias and MSE for small *n*, especially for *a* and *k*. This suggests that estimation becomes more challenging for heavier-tailed configurations, particularly when shape parameters are large.
- 5.Across both parameter settings, the bias of \hat{a} remains negative as n increases, implying a slight tendency for underestimation. This asymptotic bias, however, becomes negligible for large n, consistent with the regularity conditions of MLE.
- 6.Overall, the simulation validates the robustness of the MLE approach for the B-SIOR-R model, with estimators improving in accuracy and precision as *n* grows.

The visual display of above realization is presented in Figure (6) and Figure (7)



Table 3: Simulation results of the B-SIOR-R model for two set of parameters with sample sizes n = 25,100,200,300...,1000

n	Parameter	Set 1: <i>a</i> =	0.5, b = 3.2, k	$= 1.5, \sigma = 1$	Set 2: $a = 0.1$	1, b = 2.5, k = 1	$\sigma = 1$
		MLE	Bias	MSE	MLE	Bias	MSE
	a	0.661867	0.161867	0.93661126	0.07493826	-0.02506174	0.00974080
25	b	3.687479	0.4874786	0.98352810	2.94996100	0.44996052	1.16622795
23	k	2.382346	0.882346	3.84482432	1.55813790	0.55813786	2.19986134
	σ	1.080572	0.080572	0.02880335	1.08529500	0.08529506	0.03085520
	а	0.417977	-0.0820221	0.14335702	0.07720443	-0.02279557	0.00288960
100	b	3.414659	0.2146586	0.34931348	2.65772100	0.15772148	0.25050533
100	k	1.873237	0.3732368	1.32025998	1.09717320	0.09717319	0.31042165
	σ	1.079085	0.0790854	0.02740497	1.07428700	0.07428677	0.02167872
	a	0.409475	-0.0905241	0.08253327	0.07572742	-0.02427258	0.00206887
200	b	3.357426	0.1574262	0.19111856	2.59929000	0.09929046	0.11172344
200	k	1.650805	0.1508051	0.51490574	1.05334070	0.05334071	0.10625081
	σ	1.070995	0.0709954	0.02340118	1.06791800	0.06791759	0.01773813
	a	0.402478	-0.0975216	0.07182602	0.07921530	-0.02078470	0.00182563
300	b	3.363094	0.1630941	0.15338601	2.59489500	0.09489550	0.07420603
	k	1.550482	0.0504824	0.20100096	1.00937580	0.00937578	0.06079639
	σ	1.071210	0.0712100	0.02264084	1.06332800	0.06332791	0.01524943
	a	0.403584	-0.0964159	0.06399571	0.07894196	-0.02105804	0.00163542
400	b	3.360333	0.1603326	0.13397941	2.59109200	0.09109225	0.06051371
	k	1.513393	0.0133931	0.15245505	1.00294390	0.00294393	0.03804186
	σ	1.068049	0.0680494	0.01986014	1.05888400	0.05888351	0.01406054
	a	0.391021	-0.1089785	0.06058656	0.07988722	-0.02011278	0.00151815
500	b	3.334710	0.1347105	0.11931137	2.57831100	0.07831146	0.05156559
	k	1.523852	0.0238519	0.11990186	0.99710610	-0.00289389	0.03199950
	σ	1.067113	0.0671133	0.01910197	1.05680300	0.05680283	0.01330671
	a	0.395594	-0.1044057	0.05871807	0.08158079	-0.01841921	0.00135500
600	b	3.346242	0.1462423	0.10712219	2.56666100	0.06666085	0.04479558
000	k	1.491816	-0.0081837	0.09480632	0.99927490	-0.00072510	0.02825301
	σ	1.067420	0.0674198	0.01861448	1.05120300	0.05120345	0.01131895
	a	0.399929	-0.1000709	0.05430074	0.08273831	-0.01726169	0.00121801
700	b	3.348320	0.1483203	0.10887423	2.56394300	0.06394332	0.03946674
, 00	k	1.481770	-0.0182299	0.07424617	0.99232670	-0.00767330	0.02295891
	σ	1.064290	0.0642897	0.01778879	1.04699300	0.04699281	0.01001685
	a	0.393559	-0.1064404	0.05401443	0.08348158	-0.01651842	0.00109950
800	b	3.343971	0.1439714	0.09719068	2.55605700	0.05605711	0.03486790
	k	1.483813	-0.0161871	0.06891458	1.00105760	0.00105760	0.02067486
	σ	1.064466	0.0644664	0.01708551	1.04215500	0.04215467	0.00833130
	a	0.387923	-0.1120763	0.05287167	0.08327538	-0.01672462	0.00111471
900	b	3.338722	0.1387223	0.09415482	2.55969100	0.05969097	0.03184306
	k	1.482334	-0.0176662	0.05607478	0.99712851	-0.00287154	0.01839503
	σ	1.065703	0.0657032	0.01741942	1.04308300	0.04308289	0.00873949
	a	0.389573	-0.1104268	0.05235272	0.08260628	-0.01739372	0.00118446
1000	b	3.338444	0.1384444	0.09206825	2.55967700	0.05967745	0.03034334
1000	k	1.480102	-0.0198976	0.05618226	0.99107770	-0.00892229	0.01698761
	σ	1.064938	0.0649376	0.01711560	1.04683600	0.04683634	0.00927512

7 Applications

In Table (4), data on clean-up-gradient monitoring wells (mg/L) are presented. This data is related to groundwater contaminants measurements taken to monitor and assess the effectiveness of environmental cleanup efforts [4].

Table (5) represent gauge length measurements (in mm) for a sample of 74 items, each nominally 20 mm in length. It was first analyzed by [5].

Table (6) contain mortality rate due to HIV/AIDS in Germany from year 2000 to 2020 and it is accessed from https://platform.who.int/mortality/themes/themedetails/topics/indicator-groups/indicator-groupdetails/MDB/hiv-aids.

Table (7) represents weekly death rate due to COVID-19 from 22/3/2020 to 20/12/2020 in Dominica, accessed from https://data.who.int/dashboards/covid19/data?n=c.

Table (8) contains the survival rates of COVID-19 patients in Spain from 3 March to 7 May 2020 studied by [6].

Table (9) shows the descriptive statistics for the five datasets that were employed to investigate this research. The Ground Water dataset shows extreme variability, as reflected in its large range of 7.9, large standard deviation of 1.95, and a highly right-skewed distribution with skewness of 1.60 and kurtosis of 5.01, reflecting heavy tails and a number of outliers. On the other hand, the data of Gauge Measurement appear symmetrical and steadier, as indicated by near-zero skewness of -0.15, moderate spread with standard deviation of 0.49, and no outliers that were identified. HIV/AIDS Death Rate data are rather homogeneous with minor interquartile range of 0.1590, low standard deviation of 0.1090, and mild positive skewness, indicating minimal dispersion and relatively central distribution.



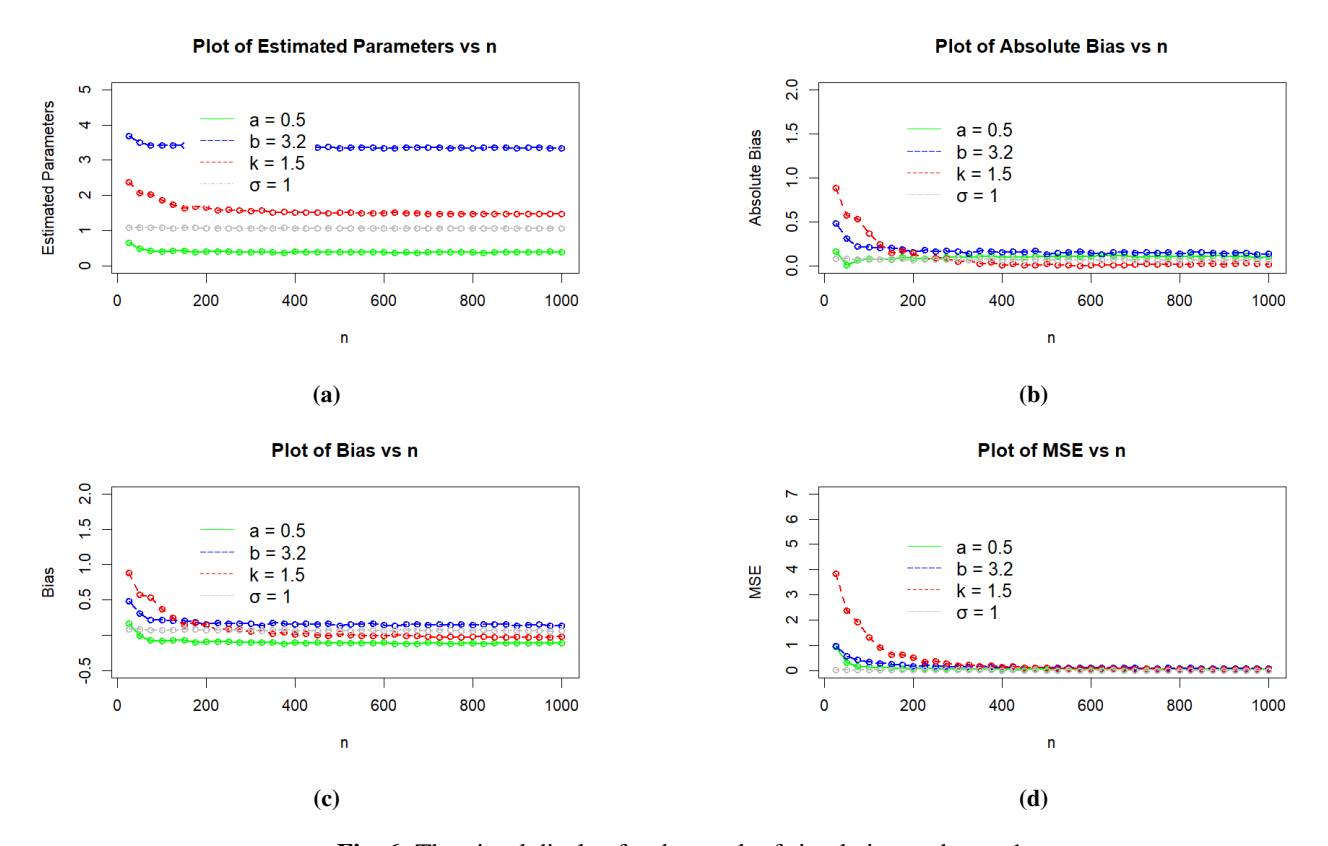


Fig. 6: The visual display for the result of simulation under set 1

Table 4: Groundwater contaminants measurements

5.1	1.2	1.3	0.6	0.5	2.4	0.5	1.1	8	0.8	0.4	0.6	0.9	0.4	2	0.5	5.3
3.2	2.7	2.9	2.5	2.3	1	0.2	0.1	0.1	1.8	0.9	2	4	6.8	1.2	0.4	0.2

Table 5: Gauge length measurements (in mm) for a sample of 74 items

1.312	1.314	1.479	1.552	1.700	1.803	1.861	1.865	1.944	1.958	1.966	1.997	2.006
2.021	2.027	2.055	2.063	2.098	2.140	2.179	2.224	2.240	2.253	2.270	2.272	2.274
2.301	2.301	2.359	2.382	2.382	2.426	2.434	2.435	2.478	2.490	2.511	2.514	2.535
2.554	2.566	2.570	2.586	2.629	2.633	2.642	2.648	2.684	2.697	2.726	2.770	2.773
2.800	2.809	2.818	2.821	2.848	2.880	2.809	2.818	2.821	2.848	2.880	2.954	3.012
3.067	3.084	3.090	3.096	3.128	3.233	3.433	3.585	3.585				

Table 6: Mortality rate due to HIV/AIDS in Germany

0.70570244	0.65946256	0.62801346	0.6143952	0.61453596	0.59540885	0.61190438
0.56040019	0.53945593	0.52641369	0.55652406	0.56615856	0.50050448	0.49723726
0.47911586	0.3270769	0.34298934	0.35461942	0.37625366	0.41652161	0.45295061

The COVID-19 Death Rate values are skewed to the right (skewness = 1.08) with low values of central tendency and a very small standard deviation of 0.0136, but there are three outliers which show some

abnormalities in deaths by region or time. On the other hand, the COVID-19 Survival Rate is mildly skewed to the left (skewness = -0.70) with moderate spread and no outliers apparent, which shows a smoother trend in



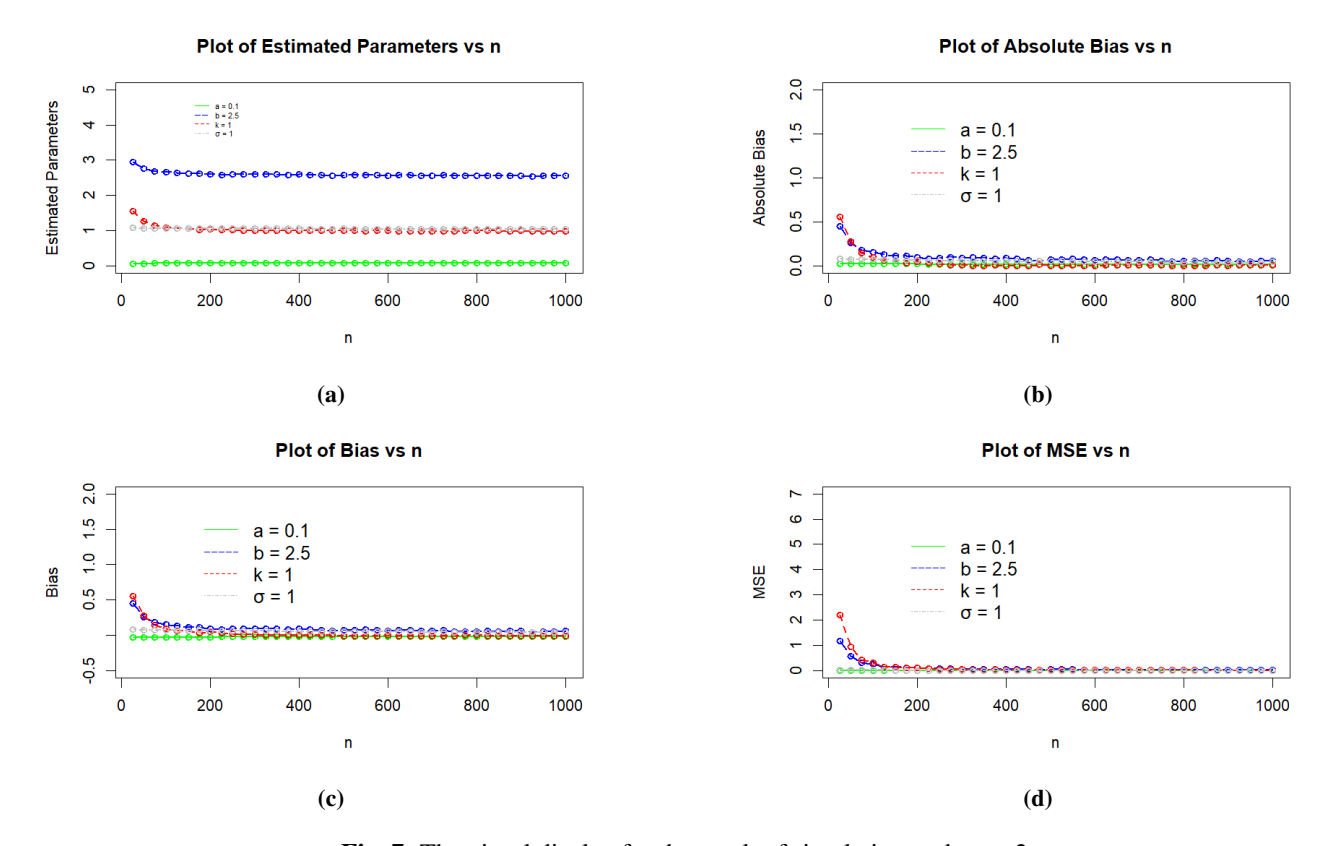


Fig. 7: The visual display for the result of simulation under set 2

Table 7: Weekly death rate due to COVID-19 in Dominica

0.029850746	0.035363458	0.05292172	0.051236749	0.053061224	0.035197989
0.032082324	0.025607639	0.01929982	0.012975779	0.016090105	0.016615654
0.012140954	0.024329382	0.01301384	0.012219227	0.013564214	0.010826889
0.008958089	0.010932598	0.016161891	0.02201862	0.023125997	0.037598736
0.033069307	0.02618165	0.019748264	0.015044519	0.011788481	0.009540117
0.009618688	0.008082768	0.008333333	0.006851922	0.005307263	0.005720572
0.004095843	0.003398641	0.002529511	0.004015331		

Table 8: Survival rates of COVID-19 patients in Spain

0.6670	0.5000	0.5000	0.4286	0.7500	0.6531	0.5161	0.7895	0.7689	0.6873	0.5200
0.7251	0.6375	0.6078	0.6289	0.5712	0.5923	0.6061	0.5924	0.5921	0.5592	0.5954
0.6164	0.6455	0.6725	0.6838	0.6850	0.6947	0.7210	0.7315	0.7412	0.7508	0.7519
0.7547	0.7645	0.7715	0.7759	0.7807	0.7838	0.7847	0.7871	0.7902	0.7934	0.7913
0.7962	0.7971	0.7977	0.8007	0.8038	0.8289	0.8322	0.8354	0.8371	0.8387	0.8456
0.8490	0.8535	0.8547	0.8564	0.8580	0.8604	0.8628	0.6586	0.7070	0.7963	0.8516

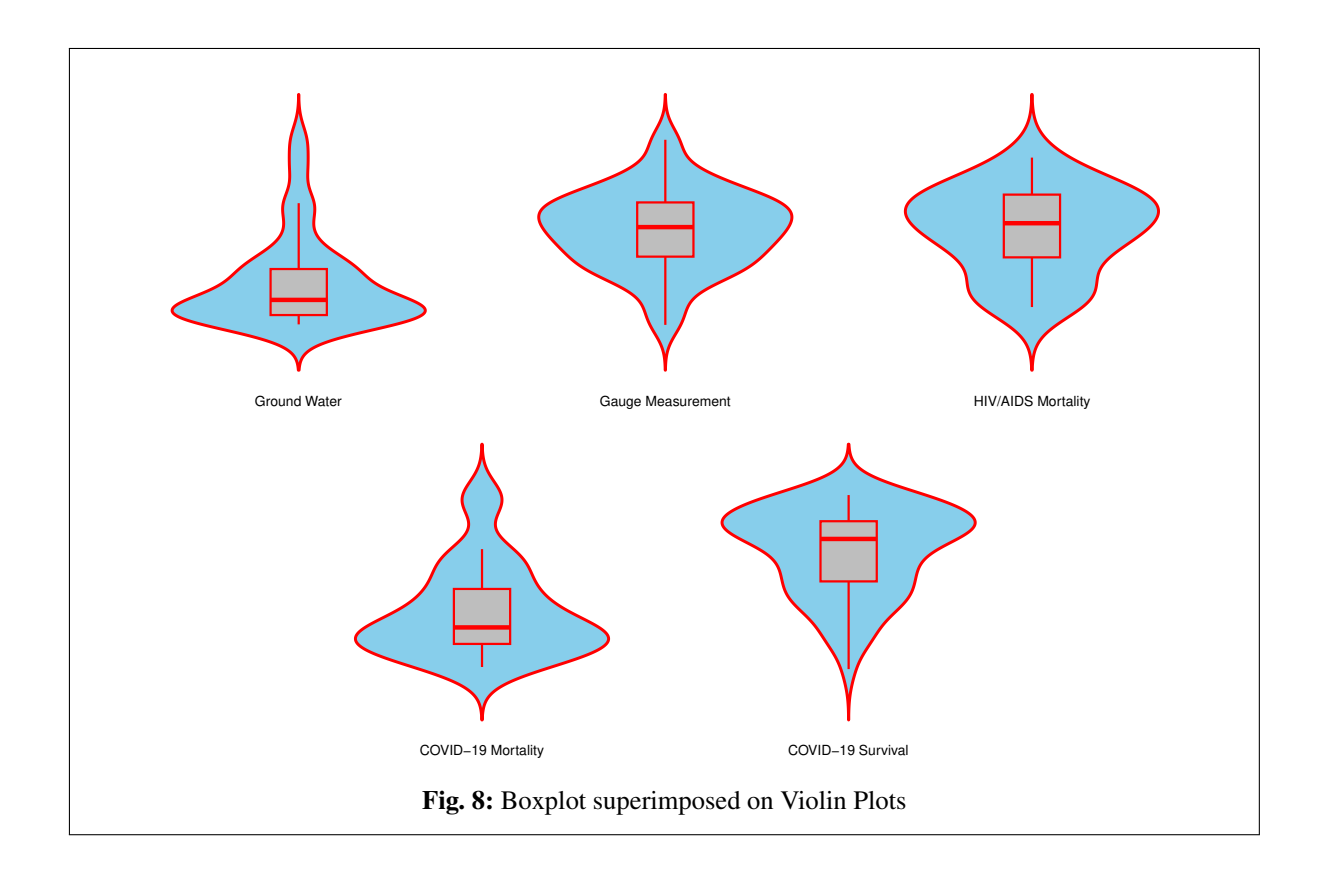
survival rates. Overall, while distributions vary across datasets, the shape characteristics such as skewness and kurtosis provide us with hints on their underlying shapes, with Ground Water data being most heterogeneous and HIV/AIDS Death Rate and Survival Rate datasets being more homogeneous and symmetric.

Figures (8-13), represent the box in violin plot, density on histogram, empirical cum B-SIOR-R CDF, empirical cum B-SIOR-R survival function, TTT plot, PP plot and QQ plot for the five different datasets. The boxplots depict that there are outliers in groundwater and COVID-19 data. All the TTT plots show increasing failure rate.



Table	9.	Ra	sic	Sta	tistics	for	the	Data	sets

Data	n	Q_1	Q_3	IQR	Outlier	Mean	Median	Var	SD	Range	Skewness	Kurtosis
Ground Water	34	0.5	2.4750	1.9750	8, 6.8	1.8794	1.1500	3.8126	1.9526	7.9000	1.6037	5.0054
Gauge Measurement	74	2.1498	2.8158	0.6660	-	2.4773	2.5125	0.2378	0.4877	2.2730	-0.1542	2.9512
HIV/AIDs Death Rate	21	0.4530	0.6119	0.1590	-	0.5203	0.5395	0.0119	0.1090	0.3786	0.1590	2.1101
					0.0529							
COVID-19 Death Rate	40	0.0094	0.0258	0.0164	0.0512	0.0190	0.0143	0.0002	0.0136	0.0505	1.0777	3.4169
					0.0531							
COVID-19 Survival Rate	66	0.6474	0.7976	0.1502	-	0.7240	0.7533	0.0118	0.1086	0.4342	-0.7049	2.6021



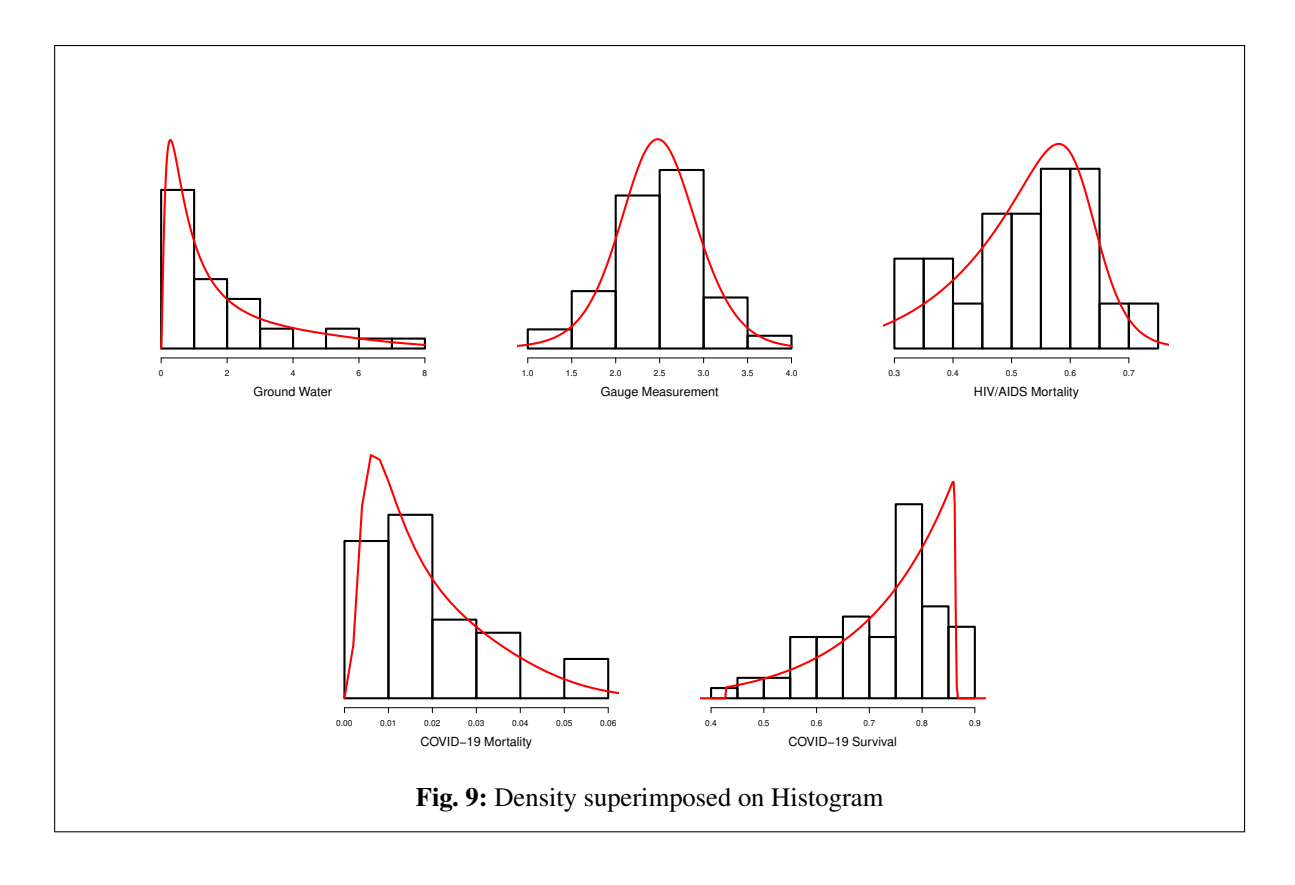
Other related distributions are juxtaposed to with the proposed B-SIOR-R model. The models are Kumaraswamy bell-rayleigh (KwBR) distribution by [7], Rayleigh distribution by [2], type-I heavy-tailed rayleigh (TIHTR) distribution by [8], gamma distribution by [9], Weibull distribution by [10], Gumbel distribution by [11], and log-normal (Lnorm) distribution by [12].

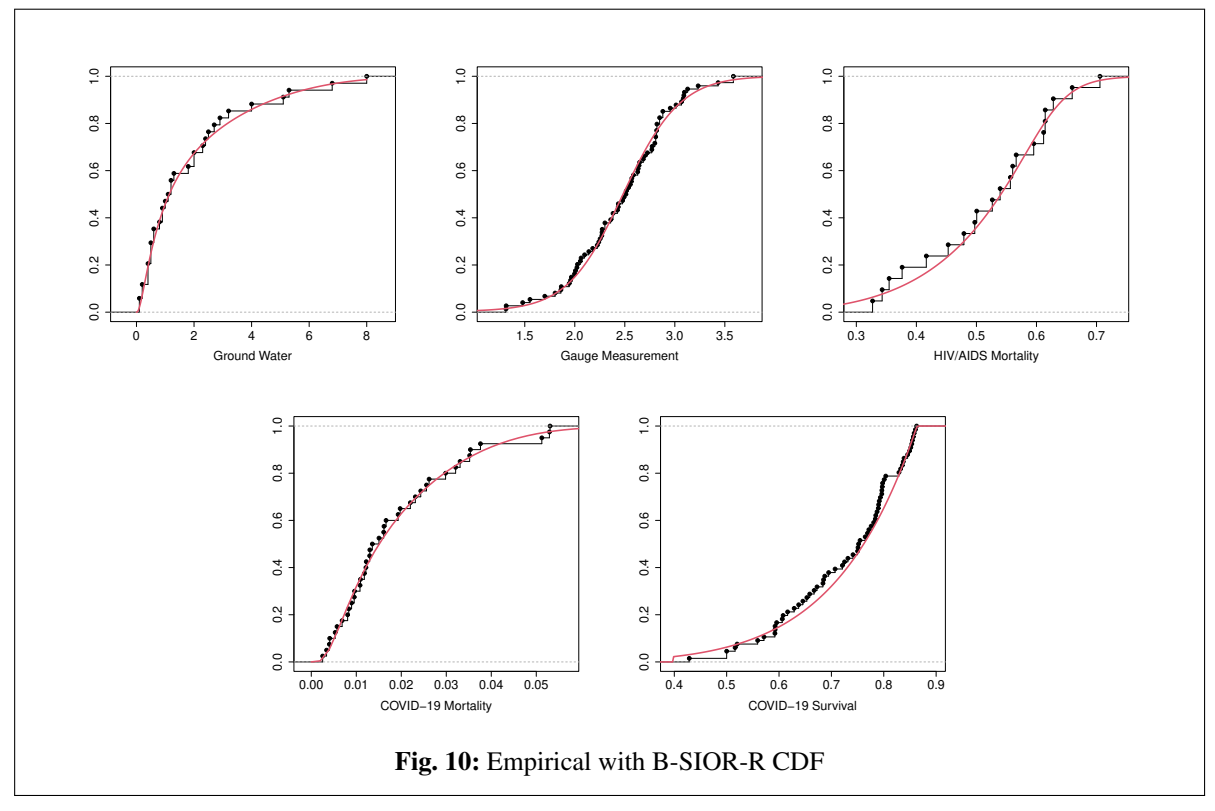
Based on Table (10), the performance of certain statistical distributions was compared across five datasets: Groundwater Measurement, Gauge Length Measurement, HIV/AIDS Mortality, COVID-19 Mortality, and COVID-19 Survival. The metrics used for evaluation are log-likelihood (LL), Akaike Information Criterion (AIC), Corrected Akaike Information Criterion (CAIC), Bayesian Information Criterion (BIC), Hannan–Quinn Information Criterion (HQIC), Anderson–Darling (A), Cramér–von Mises (W), Kolmogorov–Smirnov (KS) statistic, and the corresponding *p*-value.

In most data sets, KwBR possessed the greatest log-likelihood and lowest information criteria values, which is very good goodness of fit. However, it always produced extremely low p-values (often 2.2×10^{-16}), which is indicative of overfitting or poor fit based on the KS test. For instance, with the Groundwater Measurement data, KwBR possessed the best AIC value of -199.92, yet its KS p-value of 2.2×10^{-16} is statistically negligible.

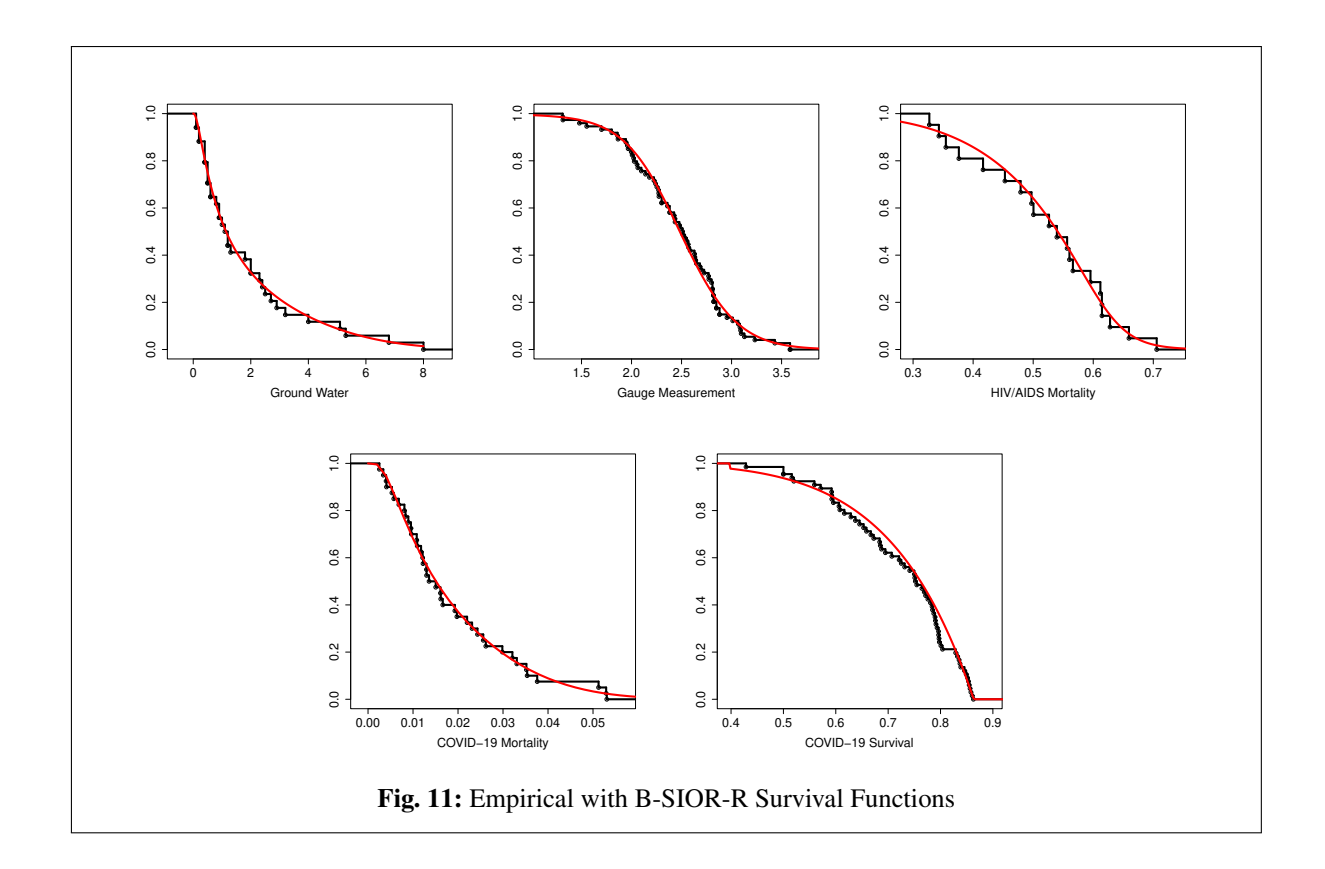
In contrast, the B-SIOR-R distribution yielded alternative information criteria values along with consistently high *p*-values across all datasets—0.9900, 0.9543, 0.9965, 0.9966, and 0.3105—displayed its statistical sufficiency and reliability both on likelihood-based and non-parametric criteria. To be precise, in the COVID-19 Mortality and HIV/AIDS Mortality datasets, not only did B-SIOR-R yield low AIC values (-240.94 and -27.45, respectively), but it also

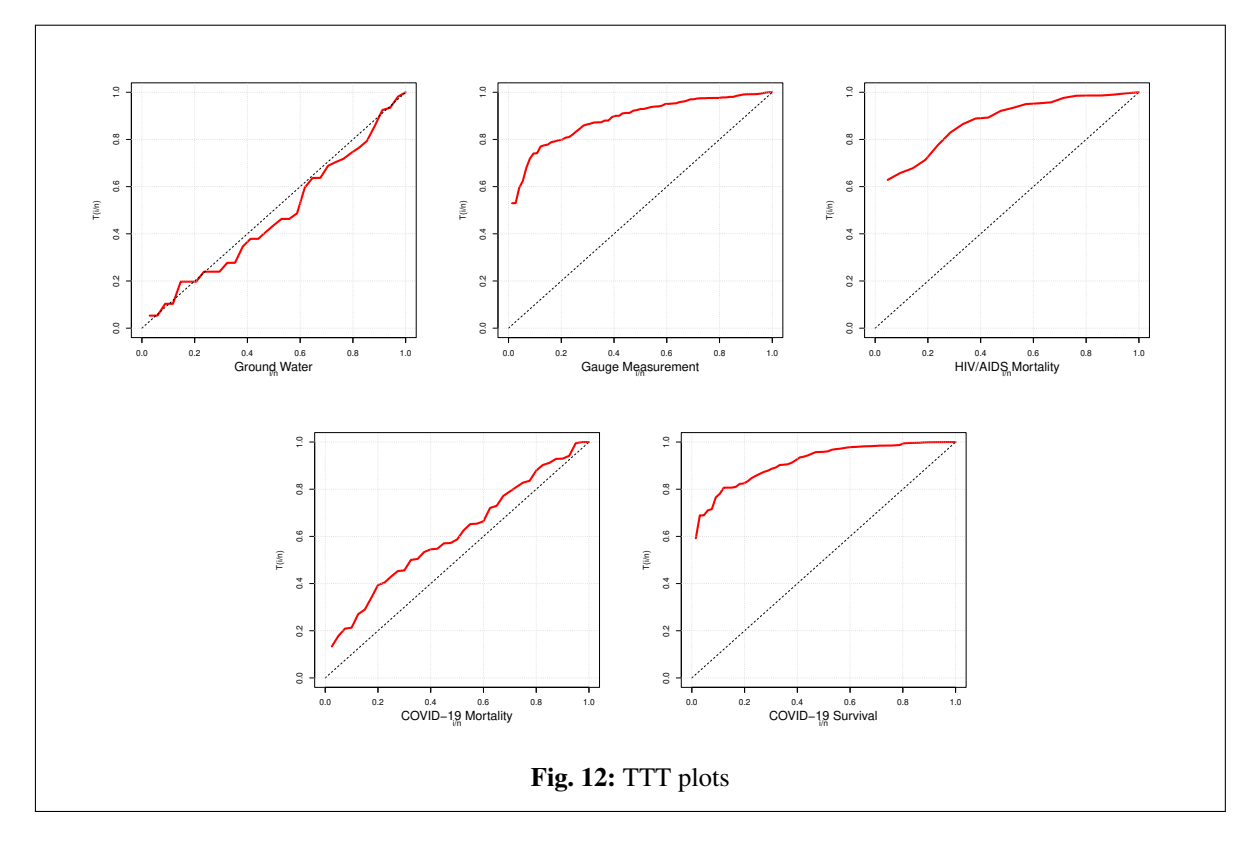




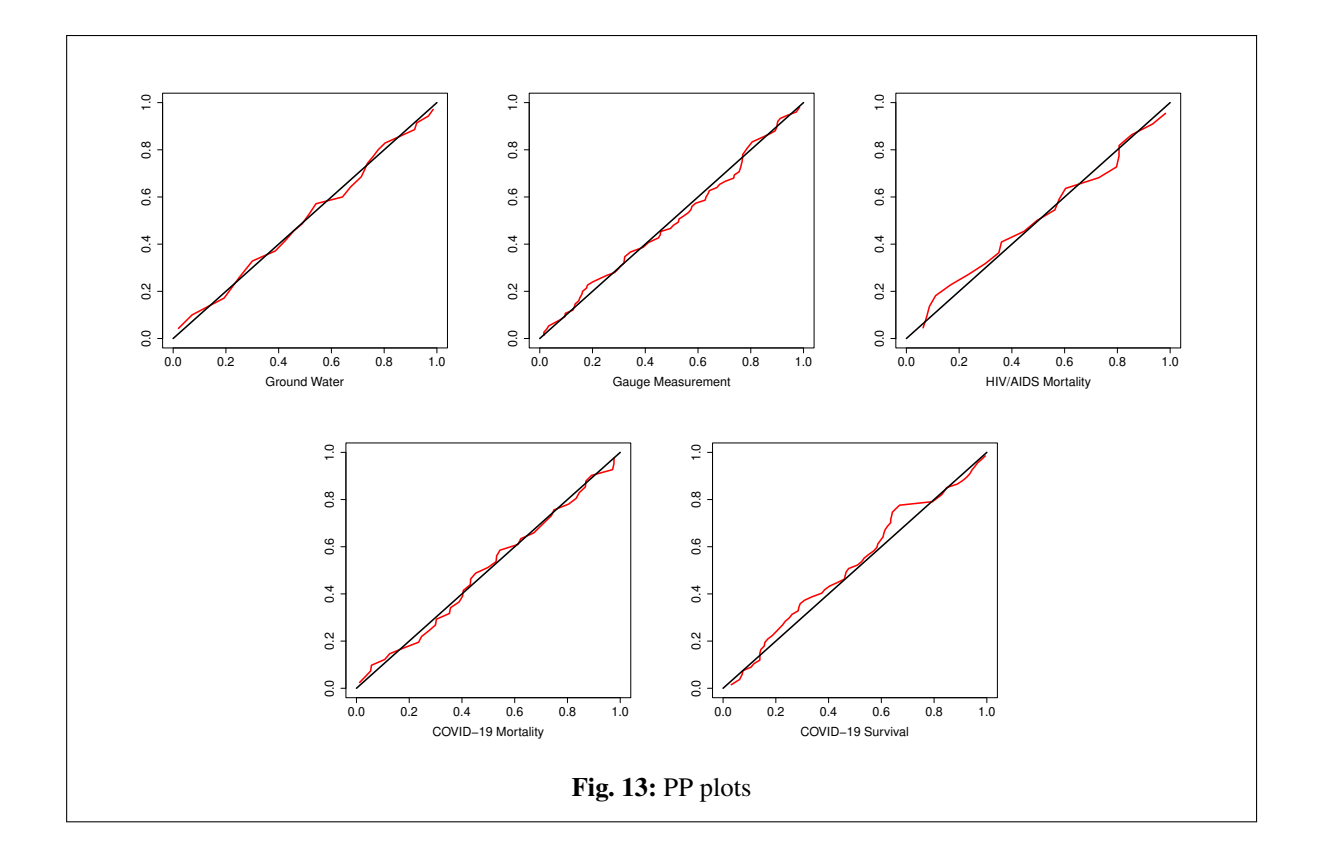












outperformed most of its competitors in goodness-of-fit tests.

Old-fashioned distributions like Weibull, Gamma, and Log-normal generally worked quite well with a reasonable balance between interpretability and quality of fit. For example, on the Gauge Length Measurement dataset, the Weibull distribution had an AIC of 107.07 and KS *p*-value of 0.8888, which indicates a reasonable fit.

Briefly, while the best likelihood-based measures are provided by KwBR, its worst KS test is a sign of a poorer practical fit. B-SIOR-R is a close rival with low information criteria combined with high performance on tests of distributions, thereby being statistical precise and practically relevant across different data contexts.

The results in Table (11) are the maximum likelihood estimates and standard errors of the models fitted to five datasets. For Groundwater and Gauge measurements, both B-SIOR-R and KwBR models produced unstable and extreme parameter estimates with huge standard errors, which may suggest issues of overparameterization or identifiability. In contrast, the older models like Weibull and Lognormal produced more stable estimates with relatively lower standard errors, reflecting better model goodness of fit. Similarly, for the HIV/AIDS Mortality and COVID-19 Mortality data sets, the B-SIOR-R and KwBR models again recorded either extreme values or undefined standard errors, while the Weibull, Gumbel, and Lognormal models were more reliable. Surprisingly, in certain cases, the Lognormal model had negative scale estimates, which might be indicative of transformation or estimation issues. In the case of the COVID-19 Survival data, this pattern existed, with B-SIOR-R and KwBR having very high uncertainty, and the Weibull and Lognormal models having more reasonable estimates. Overall, while B-SIOR-R and KwBR are flexible, estimation problems limit practical application, especially compared to the consistency and stability of the standard distributions.

8 Final Remarks and Future Work

The distribution of B-SIOR-R, as conceived in this research study, adequately extends the Rayleigh model by including Burr III scaling and inverse odds ratio transformation. Together, they offer an extremely elastic distribution with improved tail flexibility and hazard rate performance, rectifying some of the weaknesses observed in conventional Rayleigh-based models. Analytical derivations of its statistical attributes, such as entropy, extropy, and mean residual life, reaffirm it as mathematically tractable. The simulation experiment confirms the accuracy and consistency of the MLEs, particularly when the sample size increases. The B-SIOR-R model under the GASP design also enhances its usability in quality control and reliability tests. Its



Table 10: Metrics for Model Performance and Goodness of Fit

Data	Distribution	LL	AIC	CAIC	BIC	HQIC	W	A	KS	p-value
	B-SIOR-R	-54.18	116.3569	117.7362	122.4624	118.4391	0.0230	0.1727	0.0756	0.9900
	KwBR	85.81	-199.9203	-198.5409	-193.8148	-197.8381	0.2814	1.9492	0.9319	2.2×10^{-16}
	R	-74.59	151.1833	151.3083	152.7097	151.7038	0.1011	0.6556	0.3799	0.0001
Groundwater	TIHTR	-68.13	140.2667	140.6538	143.3194	141.3078	0.0717	0.4647	0.3996	3.848×10^{-5}
Measurement	Gamma	-55.41	114.8263	115.2134	117.8790	115.8674	0.0459	0.2975	0.0973	0.9044
	Weibull	-55.45	114.8992	115.2863	117.9520	115.9403	0.0463	0.3001	0.0918	0.9366
	Gumbel	-62.23	128.4557	128.8428	131.5085	129.4968	0.1633	1.0407	0.1569	0.3724
	Lnorm	-55.20	114.4088	114.7959	117.4615	115.4498	0.0311	0.2361	0.0868	0.9598
	B-SIOR-R	-52.17	111.8586	112.4383	121.0749	115.5351	0.0403	0.2526	0.0597	0.9543
	KwBR	457.16	-986.0855	-985.5058	-976.8692	-982.4090	-	-	1.0000	2.2×10^{-16}
	R	-94.15	190.3016	190.3571	192.6056	191.2207	0.0578	0.3868	0.3393	7.946×10^{-8}
Gauge Length	TIHTR	-76.51	157.0217	157.1907	161.6299	158.8600	-	-	1.3425	2.2×10^{-16}
Measurement	Gamma	-53.17	110.3300	110.4990	114.9381	112.1683	0.0871	0.5718	0.0681	0.8825
	Weibull	-51.53	107.0681	107.2371	111.6763	108.9064	0.0272	0.2425	0.0675	0.8888
	Gumbel	-58.59	121.1722	121.3412	125.7803	123.0105	0.2110	1.3639	0.0956	0.5083
	Lnorm	-54.87	113.7451	113.9141	118.3532	115.5834	0.1297	0.8464	0.0808	0.7196
	B-SIOR-R	17.7	-27.4517	-24.9517	-23.2736	-26.5449	0.0229	0.1964	0.0823	0.9965
	KwBR	161.51	-467.435	-464.935	-463.2569	-466.5283	1.6286	7.8780	1.0000	2.2×10^{-16}
	R	5.94	-9.8740	-9.6635	-8.8295	-9.6474	0.0676	0.4480	0.3157	0.0233
HIV/AIDs	TIHTR	10.76	-17.5284	-16.8618	-15.4394	-17.0751	-	-	1.6794	2.2×10^{-16}
Mortality	Gamma	16.69	-29.3856	-28.7189	-27.2965	-28.9322	0.0826	0.5336	0.1280	0.8391
	Weibull	17.79	-31.5739	-30.9073	-29.4849	-31.1206	0.0326	0.2473	0.1000	0.9710
	Gumbel	15.4	-26.8009	-26.1342	-24.7118	-26.3475	0.1297	0.7978	0.1441	0.7232
	Lnorm	16.25	-28.4934	-27.8268	-26.4044	-28.0401	0.1008	0.6366	0.1357	0.7855
	B-SIOR-R	123.18	-240.9420	-239.7992	-234.1865	-238.4995	0.0226	0.1753	0.0606	0.9966
	KwBR	122.92	-235.9403	-236.7974	-231.1847	-235.4977	0.0543	0.3507	0.0958	0.8225
	R	119.42	-236.8491	-236.7438	-235.1602	-236.2384	0.0799	0.5112	0.2118	0.0472
COVID-19	TIHTR	121.88	-239.7591	-239.4348	-236.3813	-238.5378	0.0557	0.3589	0.2561	0.0084
Mortality	Gamma	123.51	-243.0156	-242.6913	-2396378	-241.7943	0.0346	0.2328	0.0843	0.9157
	Weibull	122.97	-241.9478	-241.6235	-238.5701	-240.7266	0.0543	0.3501	0.0955	0.8257
	Gumbel	121.26	-238.5247	-238.2004	-235.1470	-237.3034	0.0752	0.4787	0.1110	0.6664
	Lnorm	123.32	-242.6429	-242.3185	-239.2651	-241.4216	0.0247	0.2097	0.0565	0.9988
	B-SIOR-R	64.23	-122.3444	-121.6886	-113.5858	-118.8834	0.0809	0.5317	0.1187	0.3105
	KwBR	501.73	-1152.3670	-1151.712	-1143.609	-1148.906	4.7935	22.3633	0.9849	2.2×10^{-16}
GOVER :	R	-1.19	4.3839	4.4464	6.5735	5.2491	0.2948	1.7345	0.3742	1.883×10^{-8}
COVID-19	TIHTR	16.09	-28.1725	-27.9820	-23.7932	-26.4420	-	-	1.2252	2.2×10^{-16}
Survival	Gamma	50.68	-97.3529	-97.1624	-92.9736	-95.6224	0.3262	1.9182	0.1554	0.0824
	Weibull	57.60	-111.1991	-111.0086	-106.8198	-109.4686	0.1594	0.9663	0.1069	0.4379
	Gumbel	43.29	-82.5715	-82.3811	-78.1922	-80.8411	0.4755	2.7832	0.1718	0.0407
	Lnorm	49.01	-94.0277	-93.8372	-89.6484	-92.2972	0.3627	2.1315	0.1617	0.0634

good fit for a large number of real data covering environmental monitoring to epidemiological mortality and survival data is a confirmation of its generality.

Despite its good performance in some areas, the B-SIOR-R model and the KwBR model yielded unstable and outlier parameter estimates with large standard errors in some datasets like Groundwater and COVID-19 Survival. This instability, as pointed out as potential issues of overparameterization or identifiability, is contrary to the stable and more robust estimates of previous models like Weibull and Lognormal. Generally, while the B-SIOR-R model is statistically resilient and flexible, it is limited in application by such estimation challenges, particularly when compared to the stability of standard distributions.

This research not only contributes a robust statistical model to the literature, but also sets the stage for future research in flexible parametric modeling for censored and asymmetric data structures.

References

- [1] Yang, H., Huang, M., Chen, X., He, Z., & Pu, S. (2024). Enhanced Real-Life Data Modeling with the Modified Burr III Odds Ratio–G Distribution. *Axioms*, 13(6), 401. doi:10.3390/axioms13060401
- [2] Rayleigh, L. (1880). XII. On the resultant of a large number of vibrations of the same pitch and of arbitrary phase. *The London, Edinburgh, and Dublin Philosophical Magazine and Journal of Science, 10*(60), 73–78. doi:10.1080/14786448008626893



Table 1	1. N	AT Do	:+b	Ctondone	Гинова	:	Parenthesis
Table I		VII.H.S	W/1fh	Standard	LErrors	1n	Parenthesis

Data	Distribution B-SIOR-R	$\begin{vmatrix} a_{\text{shape}} \\ 0.1104(0.1510) \end{vmatrix}$	<i>b</i> _{shape} 0.4901(0.2096)	<i>k</i> _{shape} 2.6735(4.4874)	σ_{scale} 2.2754(0.8926)
	KwBR	0.4808(0.1894)	$1.0998 \times 10^3 (190.6731)$	$5.7062 \times 10^{-11} (1.2886 \times 10^{-4})$	$41.3939(2.3539 \times 10^{-3})$
Groundwater Measurement	R	_ ` ` ´	-	-	1.9017(0.1631)
	TIHTR	_	-	0.0257(0.0175)	2.9657(1.0048)
	Gamma	_	-	0.5653(0.1535)	1.0624(0.2281)
	Weibull	_	-	1.0103(0.1327)	1.8879(0.3390)
	Gumbel	_	-	1.1697(0.1741)	1.0916(0.2085)
	Lnorm	-	-	1.1198(0.1358))	0.0915(0.1920)
Gauge Length Measurement	B-SIOR-R	13.0520(21.1981)	0.0513(0.0734)	2.3928(1.9831)	0.2077(0.1494)
	KwBR	1.1342(NAN)	$3.2967 \times 10^3 (3.8302 \times 10^2)$	$1.1448 \times 10^{-5} (2.3594 \times 10^{-5})$	2.3189(NAN)
	R	_	-	=	1.7848(0.1037)
	TIHTR	_	-	0.9213(0.2357)	0.2019(0.0572)
	Gamma	_	-	9.7791(1.6133)	24.2260(3.9556)
	Weibull	_	-	5.7394(0.4929)	2.6738(0.0571)
	Gumbel	_	-	0.4929(0.0409)	2.2312(0.0608)
	Lnorm	-	-	0.2093(0.0172)	0.8864(0.0243)
	B-SIOR-R	0.0064(0.0131)	8.5701(3.9222)	0.2178(0.1382)	0.6704(0.0772)
	KwBR	145.8272(19.3801)	$6.0494 \times 10^4 (NAN)$	1.2712(0.0356)	0.2121(0.0083)
	R		-	-	0.3755(0.0410)
HIV/AIDs	TIHTR	_	-	22.5211(12.5928)	0.1875(0.1154)
Mortality	Gamma	-	-	42.2483(13.0890)	21.9803(6.7324)
	Weibull	-	-	5.8439(1.0281)	0.5630(0.0221)
	Gumbel	-	-	0.1049(0.0171)	0.4656(0.0243)
	Lnorm	-	-	0.2195(0.0339)	-0.6763(0.0479)
	B-SIOR-R	0.0660(0.0888)	0.5516(0.1289)	8.0977(11.5603)	-0.0158(0.0038)
	KwBR	0.7393(0.0901)	329.5917(1246.654)	4.6103(3.4478)	16.2273(NAN)
	R	=	=	=	0.0164(0.0013)
COVID-19	TIHTR	-	=	403.2535(444.8011)	2.4825(1.3710)
Mortality	Gamma	-	-	107.8358(25.3974)	2.0449(0.4252)
	Weibull	-	=	1.4830(0.1797)	0.0211(0.0024)
	Gumbel	-	-	0.0095(0.0012)	0.0130(0.0016)
	Lnorm	-	-	4.7613(0.0851)	-4.2293(0.1204)
COVID-19 Survival	B-SIOR-R	178.5224(384.9633)	384.2236(0.0004)	0.0054(0.0006)	0.7298(0.0004)
	KwBR	$8475.6470(1.2961 \times 10^3)$	$3536.9772(4.4043 \times 10^2)$	$2.0278(2.2630 \times 10^{-2})$	$0.2621(5.5463 \times 10^{-3})$
	R	-	-	-	0.5176(0.0319)
	TIHTR	_	-	10.3918(2.5788)	0.2102(0.0580)
	Gamma	_	-	56.4933(9.8545)	40.8992(7.0908)
	Weibull	_	-	8.6767(0.8908)	0.7684(0.0114)
	Gumbel	_	-	0.1174(0.0102)	0.6669(0.0154)
	Lnorm			0.1610(0.0140)	-0.3353(0.0198)

- [3] Ristić, M. M., & Balakrishnan, N. (2012). The gammaexponentiated exponential distribution. *Journal of statistical computation and simulation*, 82(8), 1191–1206. doi:10.1080/00949655.2011.574633
- [4] Bhaumik, D. K., Kapur, K., & Gibbons, R. D. (2009). Testing parameters of a gamma distribution for small samples. *Technometrics*, 51(3), 326–334. doi:10.1198/tech.2009.07038
- [5] Kundu, D., & Raqab, M. Z. (2005). Generalized Rayleigh distribution: different methods of estimations. *Computational statistics & data analysis*, 49(1), 187–200. doi:10.1016/j.csda.2004.05.008
- [6] Afify, A. Z., Nassar, M., Kumar, D., & Cordeiro, G. M. (2022). A new unit distribution: Properties, inference, and applications. *Electronic Journal of Applied Statistical Analysis*, 15(2), 460–484. doi:10.1285/i20705948v15n2p460
- [7] Nadir, S., Aslam, M., Anyiam, K. E., Alshawarbeh, E., & Obulezi, O. J. (2025). Group acceptance sampling plan based on truncated life tests for the Kumaraswamy

- Bell-Rayleigh distribution. *Scientific African*, 27, e02537. doi:10.1016/j.sciaf.2025.e02537
- [8] Nwankwo, M. P., Alsadat, N., Kumar, A., Bahloul, M. M., & Obulezi, O. J. (2024). Group acceptance sampling plan based on truncated life tests for Type-I heavy-tailed Rayleigh distribution. *Heliyon*, 10(19), e38150. doi:10.1016/j.heliyon.2024.e38150
- [9] Johnson, N. L., Kotz, S., & Balakrishnan, N. (1995). Continuous univariate distributions, volume 2. John wiley & sons.
- [10] Weibull, W. (1951). A Statistical Distribution Function of Wide Applicability. *Journal of Applied Mechanics*, 18(3), 293–297.
- [11] Gumbel, E. J. (1958). *Statistics of extremes*. Columbia university press.
- [12] Aitchison, J., & Brown, J. A. C. (1957). The Lognormal Distribution. Cambridge University Press.
- [13] Jones, M. C. (2004). Families of distributions arising from distributions of order statistics. *Test*, *13*, 1–43.



doi:10.1007/BF02602999

- [14] Cordeiro, G. M., & De Castro, M. (2011). A new family of generalized distributions. *Journal of statistical computation and simulation*, 81(7), 883–898. doi:10.1080/00949650903530745
- [15] Aryal, G. R., & Tsokos, C. P. (2009). On the Kumaraswamy Weibull distribution. *Journal of Statistical Theory and Applications*, 8, 507–518.
- [16] Burr, I. W. (1942). Cumulative frequency functions. *The Annals of mathematical statistics*, 13(2), 215–232.
- [17] Silva, R. B., Bourguignon, M., Leão, J., & Cordeiro, G. M. (2010). The Burr XII-Weibull distribution: A generalization of the Weibull distribution. *Statistical Papers*, 51, 43–59.
- [18] Alzaatreh, A., Lee, C., & Famoye, F. (2013). A new method for generating families of continuous distributions. *Metron*, 71(1), 63–79. doi:10.1007/s40300-013-0007-y
- [19] Tahir, M. H., & Cordeiro, G. M. (2015). A new family of distributions: The T-X family. *Journal of Statistical Computation and Simulation*, 85(7), 1353–1376.
- [20] Klein, J. P., & Moeschberger, M. L. (2003). Survival Analysis: Techniques for Censored and Truncated Data. Springer.
- [21] Lawless, J. F. (2003). Statistical Models and Methods for Lifetime Data, 2nd ed. Wiley.
- [22] Chen, X., Shi, Z., Xie, Y., Zhang, Z., Cohen, A., & Pu, S. (2024). Advancing Continuous Distribution Generation: An Exponentiated Odds Ratio Generator Approach. *Entropy*, 26(12), 1006. doi:10.48550/arXiv.2402.17294
- [23] Dodge, H. F., & Romig, H. G. (1959). Sampling Inspection Tables: Single and Double Sampling. John Wiley & Sons.
- [24] Aslam, M., & Jun, C. H. (2007). Designing of group acceptance sampling plan for truncated life tests based on the Weibull distribution. *Journal of Applied Statistics*, 34(4), 445–453.
- [25] Gupta, R. D., & Kundu, D. (2001). On designing acceptance sampling plans for truncated life tests based on the generalized exponential distribution. *Journal of Statistical Planning and Inference*, 93(1-2), 115–135.
- [26] Aksam, A., & Jun, C. H. (2009). Acceptance sampling plans for truncated life tests based on the generalized Rayleigh distribution. *Communications in Statistics—Simulation and Computation*, 38(3), 500–509.
- [27] Alam, M., & Aslam, M. (2021). Design of group acceptance sampling plans for inverse Weibull distribution using a truncated life test. *Journal of Testing and Evaluation*, 49(6), 4124–4133.
- [28] Mishra, D. K., & Dey, S. (2020). Acceptance sampling plans based on truncated life tests using flexible Weibull extension distribution. *International Journal of Quality & Reliability Management*, 37(7), 1017–1032.
- [29] Ahsan-ul-Haq, M., Al-Bossly, A., El-Morshedy, M., and Eliwa, M. S. (2022). Poisson XLindley distribution for count data: statistical and reliability properties with estimation techniques and inference. *Computational Intelligence and neuroscience*, 2022(1), 6503670.
- [30] El-Morshedy, M., Altun, E., and Eliwa, M. S. (2022). A new statistical approach to model the counts of novel coronavirus cases. *Mathematical Sciences*, *16*(1), 37–50.
- [31] Almazah, M. M. A., Almuqrin, M. A., Eliwa, M. S., El-Morshedy, M., and Yousof, H. M. (2021). Modeling extreme values utilizing an asymmetric probability function. *Symmetry*, *13*(9), 1730.

- [32] Willayat, F., Saud, N., Ijaz, M., Silvianita, A., and El-Morshedy, M. (2022). Marshall-Olkin Extended Gumbel Type-II Distribution: Properties and Applications. Complexity, 2022(1), 2219570.
- [33] Korkmaz, M. Ç., Altun, E., Alizadeh, M., and El-Morshedy, M. (2021). The log exponential-power distribution: Properties, estimations and quantile regression model. *Mathematics*, 9(21), 2634.
- [34] Haj Ahmad, H., Salah, M. M., Eliwa, M. S., Ali Alhussain, Z., Almetwally, E. M., and Ahmed, E. A. (2022). Bayesian and non-Bayesian inference under adaptive type-II progressive censored sample with exponentiated power Lindley distribution. *Journal of Applied Statistics*, 49(12), 2981–3001.
- [35] Husain, Q. N., Qaddoori, A. S., Noori, N. A., Abdullah, K. N., Suleiman, A. A., and Balogun, O. S. "New expansion of Chen distribution according to the neutrosophic logic using the Gompertz family." *Innovation in Statistics and Probability*, 1(1):60–75, 2025.
- [36] El Gazar, A. M., Ramadan, D. A., ElGarhy, M., and El-Desouky, B. S. "Estimation of parameters for inverse power Ailamujia and truncated inverse power Ailamujia distributions based on progressive type-II censoring scheme." *Innovation in Statistics and Probability*, 1(1):76–87, 2025.
- [37] Orji, G. O., Etaga, H. O., Almetwally, E. M., Igbokwe, C. P., Aguwa, O. C., and Obulezi, O. J. "A new odd reparameterized exponential transformed-X family of distributions with applications to public health data." *Innovation in Statistics* and Probability, 1(1):88–118, 2025.
- [38] Gemeay, A. M., Moakofi, T., Balogun, O. S., Ozkan, E., and Hossain, M. M. "Analyzing real data by a new heavy-tailed statistical model." *Modern Journal of Statistics*, 1(1):1–24, 2025.
- [39] Sapkota, L. P., Kumar, V., Tekle, G., Alrweili, H., Mustafa, M. S., and Yusuf, M. "Fitting real data sets by a new version of Gompertz distribution." *Modern Journal of Statistics*, 1(1):25–48, 2025.
- [40] Noori, N. A., Abdullah, K. N., and Khaleel, M. A. "Development and applications of a new hybrid Weibullinverse Weibull distribution." *Modern Journal of Statistics*, 1(1):80–103, 2025.



Okechukwu J. Obulezi is a lecturer of Statistics in the Department of Statistics, Faculty of Physical Sciences, Nnamdi Azikiwe University, Awka, Nigeria. He received his MSc and Ph.D in Statistics from Nnamdi Azikiwe University, Nigeria. His current research interests

include generalized classes of distributions, distribution theory, statistical inference, entropy, and machine learning.





Sadia **Nadir** is Senior Lecturer in Statistics International Riphah University, Pakistan. pursuing She is currently Ph.D. **Statistics** her in and holds M.Phil. an in Survey Sampling from Quaid-i-Azam University, Islamabad. In addition, she

has earned a Diploma in Professional Ethics, further enhancing her academic and professional expertise. Her research interests include survey sampling, probability distributions, Bayesian statistics, and machine learning.



Chinyere P. Igbokwe is a lecturer of Statistics in the Department Statistics, School of Science and Industrial Technology, Abia State Polytechnic, Aba, Nigeria. She is currently studying at the Department of Statistics, School Computer Science

Engineering, Lovely Professional University, Phagwara, Punjab, India. Her current research interests include generalized classes of distributions, distribution theory, time series models, statistical inference, machine and deep learning algorithms.



Gabriel O. Orji is a Ph.D Student in the Department of Statistics, Nnamdi Azikiwe University, Awka, Nigeria. He received his MSc and Ph.D in Statistics from Nnamdi Azikiwe University, Nigeria. His current research interests include generalized classes of distributions, distribution

theory, statistical inference, entropy, and machine learning.



Gaber Sallam Salem Abdalla is an Assistant Professor in the Department of Insurance Risk Management, Faculty of Business, Imam Mohammad Ibn Saud Islamic University (IMSIU), Riyadh 11432, Saudi Arabia. His

professional work focuses on insurance, risk management and actuarial science, with active participation in teaching, curriculum development, and applied research that connects academic theory with industry practice. His research interests include risk modelling, insurance economics, loss distribution analysis, and enterprise risk management. He has contributed to peer-reviewed publications and participates in academic service and collaborative projects aimed at improving insurance education and practice.



Abdoulie Faal is distinguished Lecturer Mathematics at the University of Education, The Gambia (UEG), renowned for his academic excellence and research prowess. With a strong academic foundation, he holds a Higher Teachers' Certificate (HTC) in

Mathematics (2014) and a BSc in Mathematics (2017) from University of The Gambia. He further advanced his expertise with a first MSc in Economics (2022) and a second MSc in Statistics and Data Science (2025) from the Graduate School, University of The Gambia (UTG). Currently, he is pursuing a PhD at the prestigious Yunnan University of China, expanding his knowledge and contributing to cutting-edge research.

His research interests are diverse and dynamic, focusing on Econometrics Analysis, Extreme Value Theory, Statistical Inference, and Time Series. As a prolific researcher, Abdoulie has successfully published three research articles in esteemed international journals of mathematics and engineering sciences, contributing significantly to the academic community. His dedication to teaching and research exemplifies his commitment to shaping the next generation of mathematicians and researchers.



Mohammed Elgarhy is an Associate Professor of Statistics in the Higher Institute of Administrative Sciences. He received his MSc and Ph.D. in Statistics in 2014 and 2017 from Faculty of Graduate Studies for Statistical Research, Cairo University, Egypt. His

current research interests include generalized classes of distributions, distribution theory, statistical inference, entropy, ranked set sampling, and lifetime test. He has published more than 200 research articles in reputed international journals of mathematical and engineering sciences. He is a referee and editor of mathematical journals.